UNIVERSIDADE D
COIMBRA

Leonor Coelho Gonçalves Grácio Lopes

STUDY AND SELECTION OF AN EXPANDER FOR A TEST BENCH OF A MICRO-CHP SYSTEM BASED ON ORGANIC RANKINE CYCLES

Dissertação no âmbito do Mestrado Integrado em Engenharia Mecânica na especialidade de Energia e Ambiente orientada pelo Professor Doutor José Manuel Baranda e pelo Professor Doutor João Pedro da Silva Pereira e apresentada ao Departamento de Engenharia Mecânica da Universidade de Coimbra.

setembro de 2022

1 2 9 0

FACULDADE DE CIÊNCIAS E TECNOLOGIA
UNIVERSIDADE D COIMBRA

STUDY AND SELECTION OF AN EXPANDER FOR A TEST BENCH OF A MICRO-CHP SYSTEM BASED ON ORGANIC RANKINE CYCLES

A dissertation submitted in partial fulfilment of the requirements for the degree of Master in Mechanical Engineering specialized Energy and Environment

Estudo e seleção de um expansor para uma bancada de testes de um sistema de micro-CHP baseado em ciclos orgânicos de Rankine

Author

Leonor Coelho Gonçalves Grácio Lopes

Advisors

Professor Doutor José Manuel Baranda Ribeiro

Professor Doutor João Pedro da Silva Pereira

Committee

Chair	**Professor Doutor Ricardo António Lopes Mendes**
Member	**Professor Doutor Márcio Duarte Albino dos Santos**
Advisor	**Professor Doutor José Manuel Baranda Ribeiro**

Coimbra, September 2022

“In every job that must be done, there is an element of fun. You find the fun and-snap! - the job’s a game!”

Mary Poppins

À minha família e amigos.

ACKNOWLEDGEMENTS

I would like to express my gratitude to my adviser, Professor José Baranda Ribeiro and co-adviser, Professor João Pedro da Silva Pereira, for the opportunity to work with you. I really appreciated your availability, motivation and critical thinking throughout this study.

I also would like to thank my parents for all the unconditional support and for providing me with all the necessary tools throughout my life to achieve my objectives, even when they, apparently, might not make much sense.

To my siblings, my life best friends, for their wise and realistic advice and for showing me different perspectives, always with a great sense of humour, even in the most challenging situations.

To my whole family for all the support and care throughout my life and especially these last five years. I could not have done it without you.

Finally, to my beloved friends and colleagues, for all the care, stories and memories created with you.

All of you had a tremendous impact on me and the person I am today, and I could not be more grateful.

Abstract

Over the last centuries, the planet's average temperature has been increasing exponentially, leading to the intensification of natural disasters and destroying several ecosystems. This growth is mainly due to the increasing greenhouse gas (GHG) emissions such as CO_2. Therefore, it is imperative to adopt measures to reduce the dependence on fossil fuels and, consequently, decrease GHG emissions. In addition to the use of renewable energy-based systems, the use of highly efficient devices can also be a short-term solution. Among these, Combined Heat and Power (CHP) technologies stand out. This technology can simultaneously generate thermal and electrical energy by only using one energy source. Although this technology has reached maturity on a large scale, studies on the micro-scale are lacking, and further investigation is needed. Implementing this technology on a micro-scale can benefit domestic applications, and it would have a considerable impact since 28% of the final energy consumption in Europe was spent on residential applications. For household applications (1-5 kW), the CHP systems based on Organic Rankine Cycle (ORC) appear to be the most adequate option.

Based on this statement, the Mechanical Engineering Department of the University of Coimbra (DEM-UC) implemented a test bench to study this promising technology. However, this bench has some limitations and a few missing parts, such as the expander, which is currently emulated by a throttling valve. The expander is one of the most relevant components of the ORC system, along with the evaporator. For this purpose, this study assesses: i) the study and comparison of different types of expanders available; ii) the selection of the proper expander for the test bench that, in its turn, simulates a residential CHP system; iii) development of a simplified thermodynamic model of the ORC that includes the details of the expansion processes; and iv) the design and components selection of the secondary devices required by the expander selected to its implementation (such as its lubricating system).

Regarding the first objective, one of the strategies being implemented in the scientific community is the application of HVAC or heat pump compressors to operate in reverse as an expander. After extensive research, a hermetic scroll was considered the most appropriate technology for this power scale. Moreover, the compressor ZR61KRE-TFD from Copeland was selected to work as an expander. Once this compressor needs lubrication, an external cycle was developed, so that the oil does not affect the other ORC components.

Additionally, in order to simulate the thermodynamic behaviour of the ORC, it was developed a simplified model (using Matlab®) and a semi-empirical model to study in more detail the expander. For this reason, a parametric analysis is presented where it was concluded that the oil fraction reduces the power output and increases the isentropic efficiency due to its sealing effect. Higher temperature demands diminish the specific power output. The growth of the superheating degree reduces the isentropic efficiency. By increasing the maximum pressure, there is a notable growth in the specific power output.

Keywords: Cogeneration systems, Organic Rankine cycles, Residential scale, Direct vaporization, Scroll expander.

Resumo

Ao longo dos últimos séculos, a temperatura média do planeta tem vindo a aumentar exponencialmente, levando à intensificação de catástrofes naturais e destruindo vários ecossistemas. Este crescimento deve-se principalmente ao aumento das emissões de gases com efeito de estufa (GEE), tais como o CO_2. Por conseguinte, é imperativo adoptar medidas para reduzir a dependência dos combustíveis fósseis e, consequentemente, diminuir as emissões de gases com efeito de estufa.

Para além da utilização de sistemas baseados em energias renováveis, a utilização de dispositivos altamente eficientes também pode ser uma solução a curto prazo. Entre estes, destacam-se as tecnologias de produção combinada de calor e electricidade (CHP). Esta tecnologia pode simultaneamente gerar energia térmica e eléctrica, utilizando apenas uma fonte de energia. Embora esta tecnologia tenha atingido a maturidade em grande escala, faltam estudos sobre a microescala, e é necessária mais investigação. A implementação desta tecnologia em micro-escala pode beneficiar aplicações domésticas, e teria um impacto considerável uma vez que 28% do consumo final de energia na Europa foi gasto em aplicações residenciais. Para aplicações domésticas (1-5 kW), os sistemas CHP baseados no Ciclo de Rankine Orgânico (ORC) parecem ser a opção mais adequada.

Com base nesta afirmação, o Departamento de Engenharia Mecânica da Universidade de Coimbra (DEM-UC) implementou uma bancada de ensaios para estudar esta promissora tecnologia. Contudo, esta bancada tem algumas limitações e algumas peças em falta, tais como o expansor, que é actualmente emulado por uma válvula de estrangulamento. O expansor é um dos componentes mais relevantes do sistema ORC, juntamente com o evaporador. Para este efeito, esta dissertação avalia: i) o estudo e comparação dos diferentes tipos de expansores disponíveis; ii) a selecção do expansor adequado para a bancada de ensaio que, por sua vez, simula um sistema CHP residencial; iii) o desenvolvimento de um modelo termodinâmico simplificado do ORC que inclui os detalhes dos processos de expansão; e iv) a concepção e selecção dos componentes dos

dispositivos secundários exigidos pelo expansor seleccionado para a sua implementação (tal como o seu sistema de lubrificação).

Relativamente ao primeiro objectivo, uma das estratégias que está a ser implementada na comunidade científica é a aplicação de HVAC ou compressores de bomba de calor para operar ao contrário como um expansor. Após extensa investigação, um pergaminho hermético foi considerado a tecnologia mais apropriada para esta escala de potência. Além disso, o compressor ZR61KRE-TFD da Copeland foi seleccionado para funcionar como um expansor. Uma vez que este compressor necessita de lubrificação, foi desenvolvido um ciclo externo, para que o óleo não afecte os outros componentes do ORC.

Adicionalmente, a fim de simular o comportamento termodinâmico do ORC, foi desenvolvido um modelo simplificado (utilizando Matlab®) e um modelo semi-empírico para estudar em maior detalhe o expansor. Por este motivo, é apresentada uma análise paramétrica onde se concluiu que a fracção de óleo reduz a potência e aumenta a eficiência isentrópica devido ao seu efeito selante. Temperaturas objetivo mais elevadas diminuem a potência específica de saída. O crescimento do grau de sobreaquecimento reduz a eficiência isentrópica. Ao aumentar a pressão máxima, há um crescimento notável na potência específica.

Palavras-chave: Sistemas de cogeração, Ciclos Orgânicos de Rankine, Escala Residencial, Vaporização direta, Expansor scroll.

Contents

LIST OF FIGURES

LIST OF TABLES

LIST OF SIMBOLS AND ACRONYMS/ ABBREVIATIONS

List of Symbols

Symbol	Name	Unit
$\dot{Q}$	Thermal power	kW
$\dot{W}$	ORC power output	kW_e
c_p	Heating value	$kJ/(kg.K)$
$\dot{m}$	Mass flow rate	kg/s
h	Specific enthalpy	kJ/kg
N	Rotational speed	rpm
T	Temperature	K, ℃
V	Volume	m^3
A	Area	m^2
γ	Isentropic exponent	
p	Pressure	kPa
AU	Supply heat transfer coefficient	W/K
$V_{s,exp}$	Swept volume	cm^3
s	Entropy	$kJ/(kg.K)$
v	Specific volume	
$r_{v,in}$	Buit-in volume ratio	
$\dot{V}_{s,exp}$	Volume flow rate	
$\Delta T2$	Superheating temperature	K, ℃
P	Power	kW
τ_{loss}	Mechanical loss torque	$N.m$
C_g	Oil circulating mass fraction	
η	Efficiency	$-$
θ	Water post heating fraction	%
ρ	Density	kg/m^3
X	Vapour quality	$-$
ζ_{wf}	Working fluid fraction	%

List of Indexes

Index	Name
w	Water
max	Maximum
CHE	Condenser Heat Exchanger
EHE	Evaporator Heat Exchanger
P	Pump
PH	Post Heat
su	Supply section of the expander
ex	Exhaust of the expander
$leak$	Internal leakage of the expander
$crit$	Critical
ad	Adapted
exp	Expander
sh	Shaft
s	Swept
n	Nominal
$loss$	Mechanical loss
in	Internal
e	Electrical
i	Isentropic
in	Internal
amb	Ambient
η	Efficiency
t	Two-phase
r	Refrigerant
L	Liquid
V	Vapour
oil	Oil
ref	Reference
{1, ..., 13}	Specific point in the diagram

Acronyms/Abbreviations

GHG	Greenhouse gases
NOAA	National Oceanic and Atmospheric Administration
CHP	Combined Heat and Power
ORC	Organic Rankine Cycle
ODP	Ozone Depletion Potential
GWP	Global Warming Potential
DEM-UC	Mechanical Engineering Department of the University of Coimbra
TDC	Top dead centre
HVAC	Heating, ventilation and air conditioning
BWR	Back Work Ratio

1. INTRODUCTION

1.1. Framework

Nowadays, awareness towards climate change is increasing, particularly on its causes and consequences since it has started interfering with individuals' lives. The increase in the planet's average temperature has led to the intensification of natural disasters and has destroyed various ecosystems. One of the significant contributors to this phenomenon is greenhouse gases (GHG), such as methane, nitrous oxide, carbon dioxide (natural) and fluorinated gases (synthetic). In excessive quantities, especially carbon dioxide (CO_2), these gases in the atmosphere have harmful consequences for our ecosystem [1].

According to the National Oceanic and Atmospheric Administration (NOAA) and the Oceanography Scripps Institute of the University of California in San Diego [2], the CO_2 levels in 2022 are 50% higher than the levels of the pre-industrial era (see Figure 1). Particularly, from the first Industrial Revolution, in the 18th century, until 2004, these levels increased by 35% [3]. This growth can be explained by the incessant search for new technologies associated with fossil fuels, to improve people's quality of life. Currently, the dependency on fossil fuels is still very pronounced, as shown in Figure 2 [3].

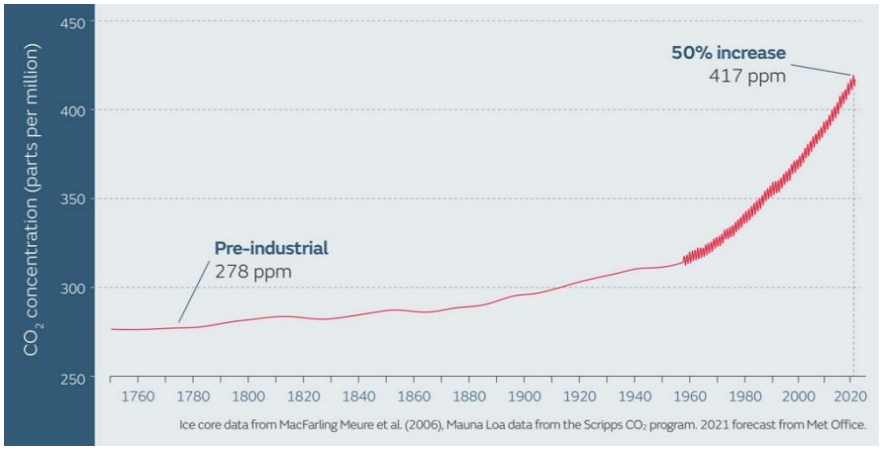

Figure 1- Atmospheric concentration of CO_2 between 1700 and 2020.

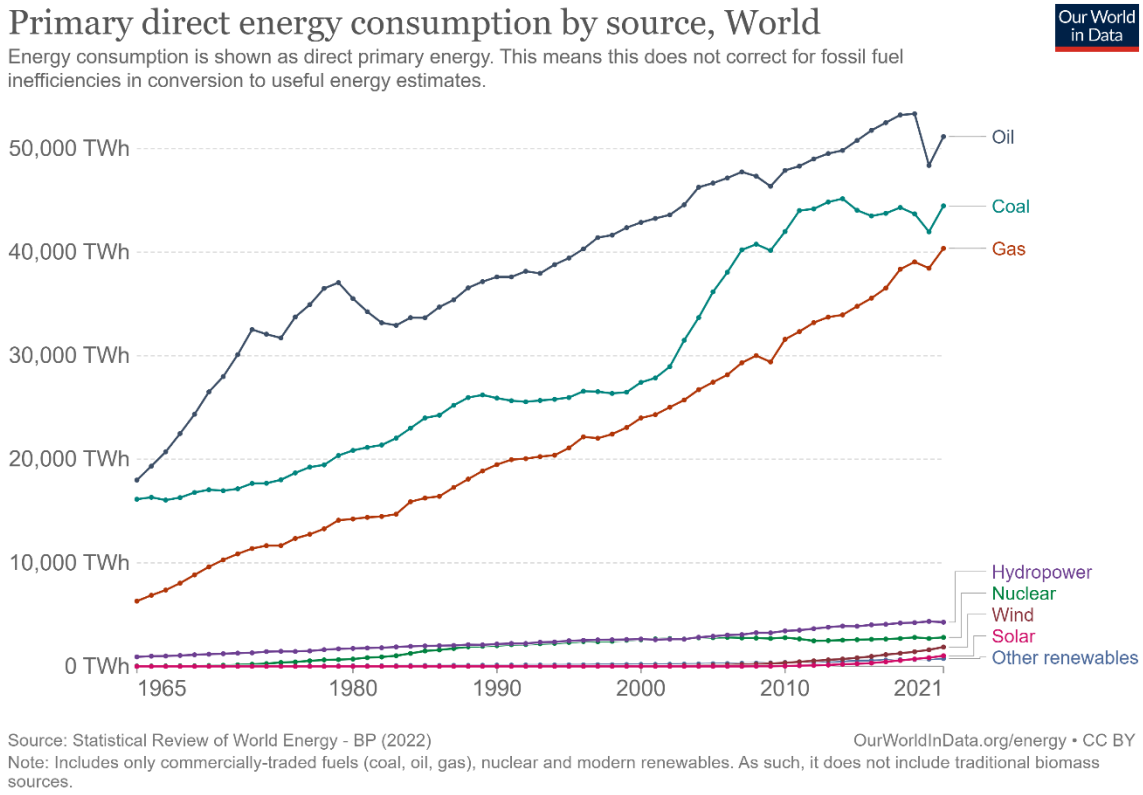

Figure 2- World's primary direct energy consumption by source between 1965 and 2021.

The intensification of energy consumption throughout the years is presented in Figure 2. The enormous increase in energy consumption can be justified not only by the population's growth but also by the exponential increase in individual energy needs [4]. Besides the high consumption of fossil fuels, there is a slight improvement in renewable energies in order to reduce CO_2 emissions and its negative consequences.

In addition to the use of renewable energy-based systems, the use of highly efficient devices can also be a solution for a short-term period. Among these, Combined Heat and Power (CHP) technologies stand out and, therefore, have received considerable attention from researchers and entrepreneurs. These systems allow the production of two types of useful energy simultaneously by using only one energy source and, in that way, reduce primary energy consumption, promoting economic savings and lowering CO_2 emissions [5]. Due to these aspects, CHP technologies are referred as a sustainable path towards the reduction of dependency on fossil fuels [6].

Even though CHP systems have been studied and implemented with success on a medium-to-large scale, studies at the small-to-micro scale are lacking, and further investigation is needed [4]. These technologies implemented at this scale can be beneficial in households' applications. According to the *Eurostat* database [7], in 2020, 28% of the final energy consumption in European Union was spent on residential applications, as shown in Figure 3. This number has been increasing over the years Thus, implementing sustainable technology options (such as CHP) in this sector could notably impact primary energy consumption [7].

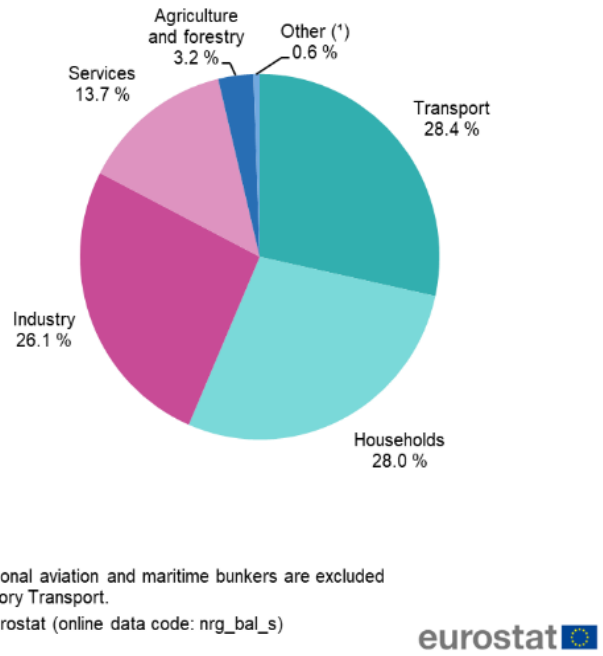

Figure 3-Final energy consumption by sector in the European Union in 2020.

There are four main groups of technologies available for CHP applications: thermophotovoltaic generators, chemical conversion systems (fuel cells), internal combustion systems (reciprocating spark ignition engines or gas micro-turbines) and external combustion systems (steam engines, Rankine or Stirling cycles). Between those, the most suitable and promising technology for the residential sector is the Rankine cycle due to its simplicity and low probability of creating difficulties in retrofitting current installed heating systems (wall-mounted conventional or combi-boilers) [4]. In addition to these aspects, Rankine based solutions presented electrical (from 6 to 19% with power size from

1-10 kW_e) and thermal efficiencies (between 77% and 90% from thermal sizes ranging of approximately 8-44 kW) adequate to residential applications. Therefore, Rankine based micro-CHP systems offers a very good alternative to standard boilers, meeting the typical residential loads [8]. However, this technology has still not reached its state of maturity and further research is needed for a wide-spread-market introduction on the residential scale.

From a technological point of view, the Rankine cycle is composed by: a pump, an evaporator, an expander and a condenser. The connections between those components are presented, with the respective energy fluxes, in a schematic representation in Figure 4. The cycle starts with the pressurization of the working fluid by the pump. Then the fluid is leaded to the evaporator where its temperature is increased until its total vaporization. From the evaporator, the working fluid goes to the expander where its pressure is reduced due to its expansion. Afterwards, the working fluid circulates to the condenser where it returns to liquid phase due to a temperature reduction caused by a heat transfer to a heat sink. Lastly, the fluid returns to the pump and the cycle restarts.

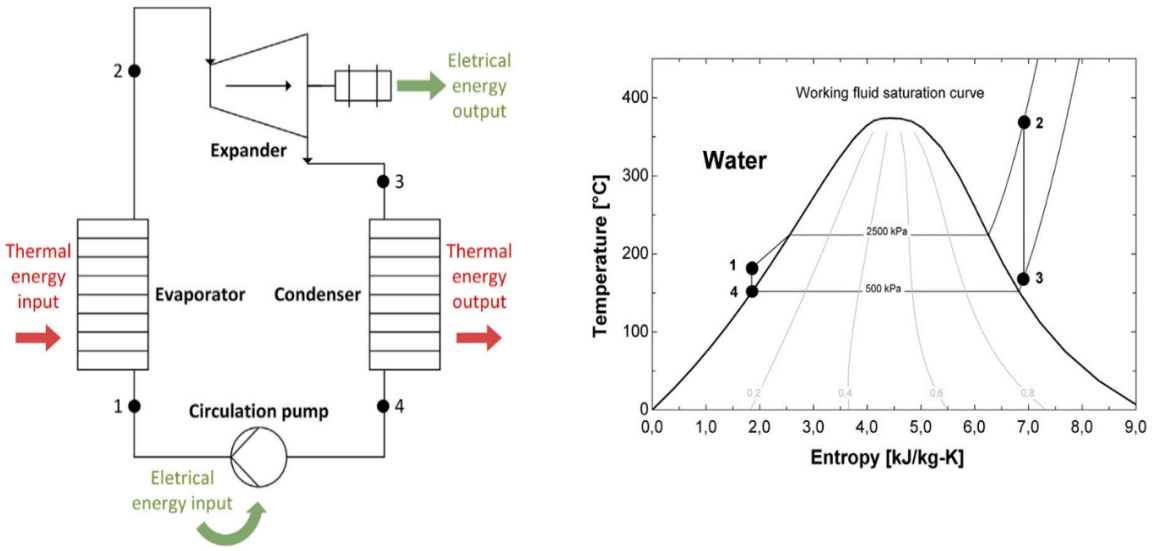

Figure 4 - Schematic representation of a Rankine cycle; T-s diagram of a water-steam cycle.

Within the Rankine technology, there are two options to be considered regarding the working fluid: water or organic solutions.

Typically, the use of water/steam solutions require high pressures and high superheating degrees which leads to additional design and manufacturing requirements and, therefore, the use of expensive and robust components. For these reasons, it can be concluded that Rankine water based systems are not the most suitable for domestic applications [4]. On the other hand, using organic fluids avoids high pressures and high superheating degrees, which can, for this reason alone, help the introduction of technology in this market [9]. To conclude this comparison, the main advantages and drawbacks of using organic fluids are shown in Table 1.

Table 1 - Advantages and drawbacks of organic fluids in Rankine solutions for domestic application [4,10].

Advantages	Drawbacks
• Low degrees of superheating, (due to its characteristic curve, see Figure 5) ensuring the maintenance of the expander and its high efficiency; • High saturation pressures to low temperature values (comparing with the water) permitting the system versatility to different heat sources; • Allows operating with low pressures, which reduces the operational risks and design requirements.	• Higher cost and lower availability; • Toxic and flammable; • Negative environmental impact (positive values of global warming potential and, possible, ozone depleting potential); • Lower chemical stability (can deteriorate with lower operating temperatures).

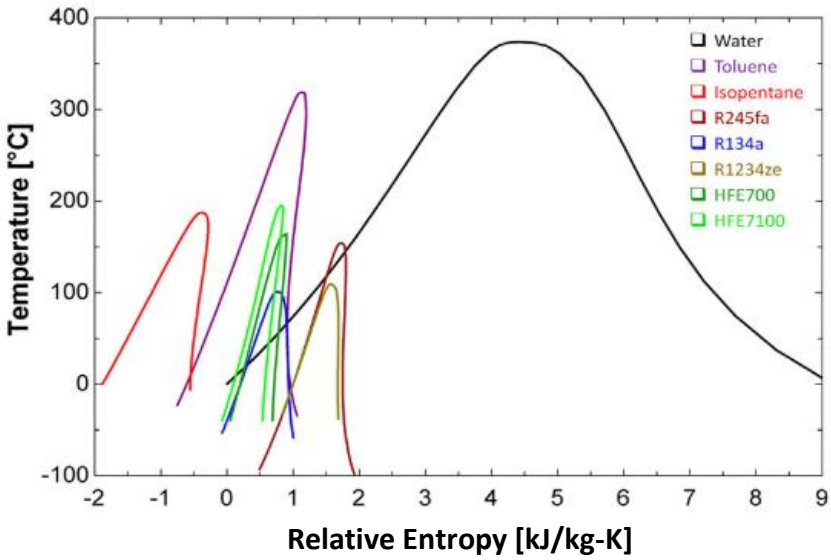

Figure 5 - Relative T-s saturation curves for the water/steam and for the most common organic fluids.

Based on the information presented, ORC is the safest, simple, and most reliable choice to be applied in domestic applications in order to retrofit the current standard heating systems and, therefore, the system chosen for the current study [4].

1.2. Status of the micro-scale ORC technology

As previously stated, ORC based micro-scale CHP systems have the potential to retrofit the current heating domestic appliances. For this reason, several research projects and studies are being developed [8]. In order to understand the current status of technology, eleven research papers were selected and deeply analysed. These papers were chosen based on their impact on the scientific community and/or their publication date. A summary of those is presented, in reverse chronological order, in Table 2, where the authors, the publication date, the ORC main components, the working fluid and the heat source are described. A complete analysis of these papers can be seen in APPENDIX A.

It is important to start mentioning that the test rigs analysed in Table 2 were implemented in a laboratory scale but always attempted to simulate some aspects or particularities of real situations.

When analysing the heat sources, some of the studies do not simulate primary energy sources, but waste heat of some applications. For example, Dumont et al. [11] uses surplus heat from a solar panel which can be adequate for households. Nevertheless, this option is dependent on the availability of the solar energy and do not promote a simple retrofit of the current installed heating devices. Another authors, such as Usman et al. [12] , Eyer et al.[13], Wajs et al. [14], and Richter et al. [15], use a boiler (electrical or gas) for the heat sources of their systems. However, their study does not focus on the operation of the entire system but only specific characteristics of it. Even if they ought to evaluate the entire system, they implemented an intermediate circuit between the heat source and the ORC evaporator. This configuration is designated in the scientific community by indirect vaporization of the organic fluid which is not recommended for domestic application because it will increase the inertia (response time), the size, and the complexity of the entire system [4].On the other

hand, studies with direct vaporization of the organic fluid for residential scale are practically non-existent due to, probably, thermal degradation issues [16].

Regarding the working fluids, the most commonly used is the R245fa. This fluid has good thermodynamic proprieties (e.g.: adequate values of saturation pressures) for this type of applications. Although its value of Ozone Depletion Potential (ODP) is zero, this organic fluid has a high level of Global Warming Potential (GWP) , thus, it will be eventually replaced by R1233zd [17]. There are also other working fluids described in Table 2 such as ethanol which is highly flammable. However, and once direct pressurization appears to be the proper path to follow, this solution is not advisable. For the condenser and the pump of the ORC, apparently there is no need of being thoroughly studied because the solutions presented in the market fulfil the technological requirements regardless the power scale.

Finally, one of the most important components of the ORC system is the expander. For this component, two main investigations have been conducted: i) the study of different types and ii) adaptation of compressors that are commonly used in the refrigeration sector. For instance, the most common one observed in Table 3 is the scroll type. For this specific market, and mainly because of price requirements, the proper path to be followed is the conversion of scroll compressors from HVAC or heat pumps unit to work as an expander in the ORC [10].

From this literature review, it can be concluded, that the expander and the evaporator are extremely important components in the cycle and still require further investigation.

Author and date	Heat Source	Working Fluid	Expander	Evaporator	Condenser
Moradi, et al. 2021 [18]	5 electrical heaters heating the diathermic oil	R134a	Lubricated scroll compressor (inverted)	Plate HX	Plate HX
Usman, et al. 2020 [12]	Steam	R245fa	Scroll expander	Braze plate HX	Braze plate HX
Weller, 2020 [19]	Not Defined	R1336mzz(E)	Piston expander	Not Defined	Not Defined
Eyer, 2019 [13]	Resistance heater is applied to the water	R1233zd(E)	Open type twin screw compressor (inverted)	Not Defined	Not Defined
Eyer, 2019 [20]	Electrical resistance heater	Not Defined	Semi-hermetic automotive scroll compressor (inverted)	One-pass coaxial tube-in HX	Air-cooled
Richter, 2018 [15]	Electric boiler simulating low-potential waste heat	R245fa	Twin-screw compressor (inverted)	Plate heat exchanger	Plate heat exchanger
Dumont, 2017 [11]	Surplus heat from solar panel	Not Defined	(hermetic) HVAC off-the-shelf scroll compressor (inverted)	Plate-type heat exchanger	Plate-type heat exchanger
Galindo, 2017 [21]	Exhaust gas line from a gasoline engine	Ethanol	Piston wash-plate	Boiler	Cooling water
Wajs, 2016 [14]	Gas boiler	1.Water; 2. Ethanol	Small size axial vapour microturbines	Heat-Exchanger with oil	Not Defined
Quoilin, 2011 [10]	2 air flows	HFC-245fa	Oil-free open drive scroll compressor (inverted)	Set of 3 heat exchangers	HX cooled by water
Quoilin, 2011 [10]	2 air flows	HFC-245fa	Hermetic lubricated scroll compressor (inverted)	Set of 3 heat exchangers	HX cooled by water

Table 2 - Resume of the proprieties of the test-rigs analysed.

1.3. Objective and Motivation

As mentioned before, one of the strategies to help mitigate climate change caused by humans can be implementing cogeneration systems based on ORC technologies in a residential application. With this in mind, the Mechanical Engineering Department of the University of Coimbra (DEM-UC) developed a test bench to simulate this kind of systems. However, this bench has some limitations and a few missing parts, such as the expander which has been currently emulated by a throttling valve.

Therefore, and being the expander one of the most crucial components (as concluded in the previous section), the motivation of this work is complementing this test bench, so it can produce thermal and electrical energy in order to become a truly micro-CHP system. Hopefully, this research is another step forward in implementing this sustainable system in residencies in the future.

For this purpose, the objectives of this work are:

i. The study and comparison of different types of expander available;
ii. The selection of the proper expander for the test bench that, in its turn, simulates a residential CHP system;
iii. Development of a simplified thermodynamic model of the ORC that includes the details of the expansion processes;
iv. Design and components selection of the secondary devices required by the expander selected such as its lubricating system.

1.4. Dissertation structure

This dissertation consists of 4 chapters, including this first introductory one and the conclusions.

Chapter 1 provides an overview of the world's climatic situation: the increase in energy demand associated with dependence on fossil fuels. To fight this climate crisis, some strategies and technologies are approached in this chapter, such as CHP systems based on the organic Rankine cycle technology. Furthermore, the analysis of this technology for the residential scale is made through the review of some pertinent and updated scientific papers.

Chapter 2 describes the selection process of the most suitable type of expanders to be applied in the test bench which starts with a theoretical investigation on the existing types that could be used in micro-scale applications and ended with the final expander definition.

Chapter 3 starts by describing the existing test bench in the Mechanical Engineering Department of the University of Coimbra. It also assesses the implementation of the selected expander and its necessary devices for the proper operation of test bench such as the lubricating system.

2. SELECTION OF THE EXPANDER

2.1. Technologies

After concluding that the expander is an essential element on the ORC performance, it is imperative to study in detail this component in order to select the most appropriate type for households' applications (1-10 kW_e).

The expansion machines can be categorised into two main categories:

- Positive displacement (volumetric) expanders;
- Velocity based expanders (turbomachinery or just designated as turbines).

Regarding these two categories, turbomachines are not considered suitable for very-small-scale units, mainly because their rotating speed increases drastically with a decreasing turbine output power. This is due to their tip speed being more or less constant, whatever the turbine size. As a consequence, when the turbine size decreases, the rotating speed increases in the same proportion[10].

In comparison, the volumetric machines are more suitable for micro-scale application due to their low cost, simplicity, low rotational speeds and tolerance to two-phase flows [12].

As previously mentioned, these systems can achieve competitive costs since the components already exist in the market and can be easily adapted to these applications. In this case, the strategy to implement volumetric expanders is to convert cooling compressors to operate as an expander. These compressors can be easily found in the market with accessible prices.

There are four main types of volumetric expanders that can be implemented: scroll, screw, piston and rotary vane. The characteristics and operation of these types are described in detailed within the next sections.

2.1.1. Rotary Vane Expander

Rotary vane expanders are positive displacement machines in which the working fluid expands as a result of changing the volume of closed spaces occurring between a rotor and a casing (sometimes designated as housing)[22]. The working fluid enters the expander at the location having a small clearance. A rotor with moveable vanes attached is near the casing in asymmetric orientation. The rotation of the rotor allows the vanes to move outwards while trapping the working fluid. As the rotation angle increases the volume bound by consecutive vanes increases and expansion of working fluid occurs. [23] This process is schematically represented in Figure 6.

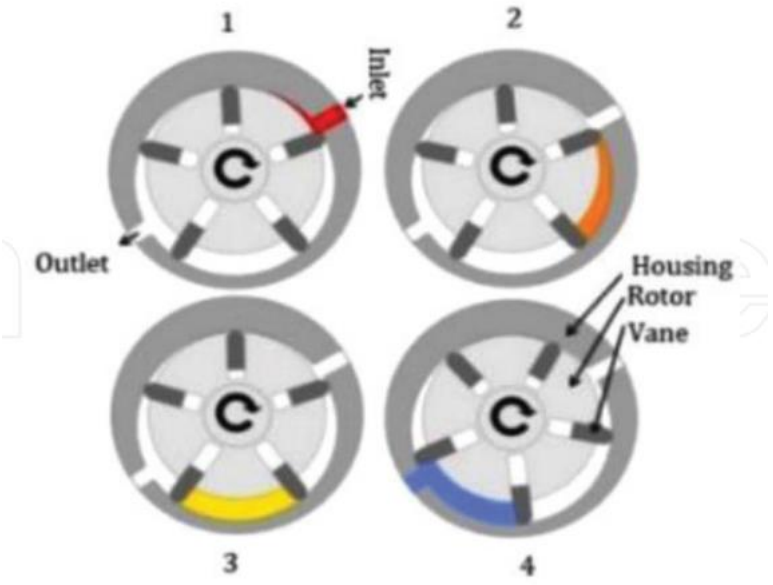

Figure 6 - Schematic representation of a rotary vane expander operation [23]**.**

There are some advantages in using this type of expanders, such as: i) present a simple, compact and reliable structure, ii) can be directly attached to the generator due to their low rotational speeds, iii) offer low production costs, iv) are available commercially, v) present small vibration and low acoustic impact.

Although these advantages there are some disadvantages that sometimes do not compensate their application, such as: i) lower isentropic efficiencies compared to other volumetric expanders, they can attain efficiencies of up to 80%, but according to other

publications these efficiencies can be just barely above 50% which is justified by leakages and higher friction losses between casing and vanes [24], ii) rotational speeds are usually lower than 1000 rpm causing the increase of the vanes due to the centrifugal forces, which increase the friction and entails the risk of overheating. In order to reduce this friction and to keep operating temperatures low, a small quantity of lubricant is used [23,24], iii) the maximum temperature inlet is limited to around 140ºC [24] and the working medium temperature is around 110ºC [22]. If a very high temperature working fluid is passing through it, the expansion of the vanes might cause them to stick and the machine will cease its operation. This limits the use of vane expanders for high-temperature applications.

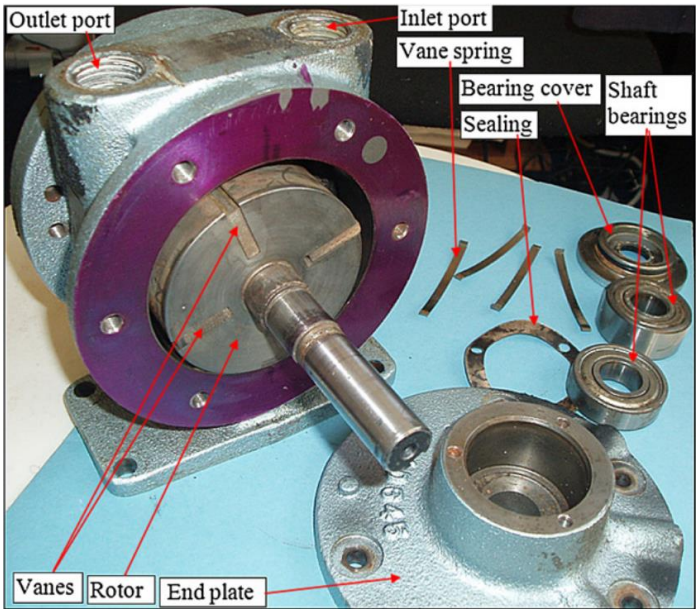

Figure 7 - Photography of a rotary vane expander with the identification of its main components [22].

2.1.2. Twin-Screw Expander

A twin-screw expander is composed of two helical rotors design with an accurate profile to trap the required amount of the working fluid. The synchronised movement of intermeshing rotors generates volume profiles with the length of the. The working fluid is expanded in that meshed chamber[22]. This can be observed in Figure 8 and Figure 9.

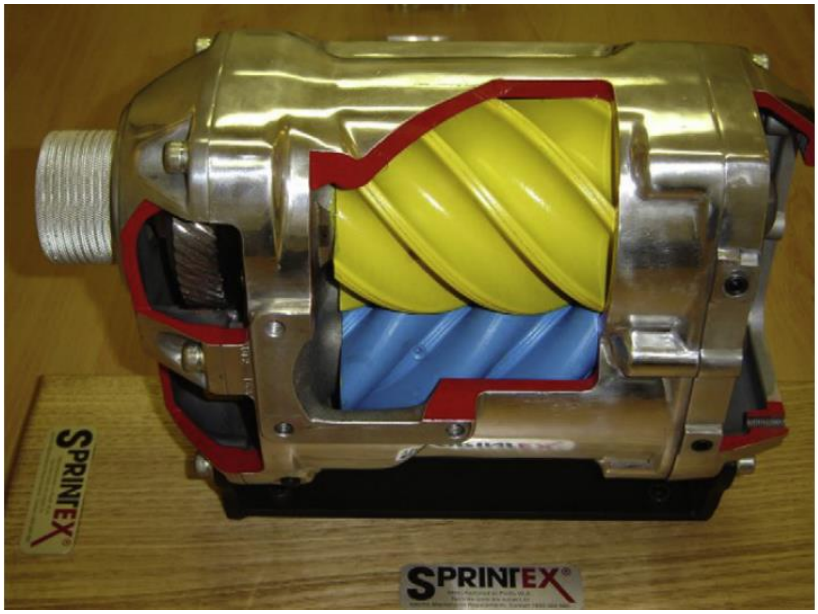

Figure 8 - Photograph of a twin-screw expander [22]**.**

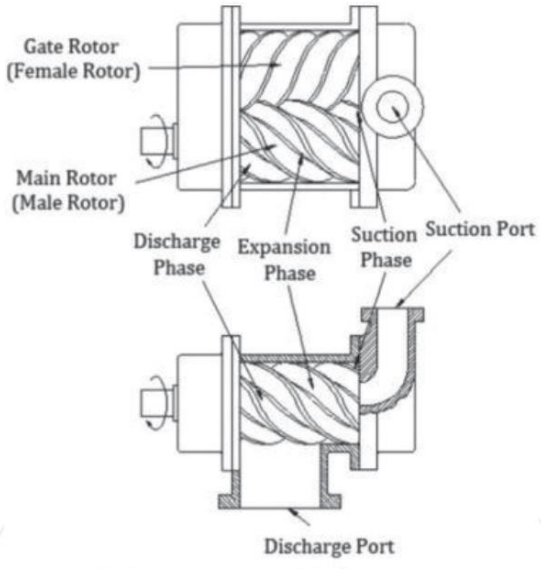

Figure 9 - Schematic representation of a twin-screw expander with the identification of its main components.

There are many advantages in the use of this type of expander. Firstly, they are capable of wet and dry expansions, with isentropic efficiencies around 70% and adiabatic efficiencies around 80% [24, 22]. Another benefit is its compactness and higher rotational

speed when compared to scroll machines [25]. Regarding the lubrication they can work as an oil-free expander however, it is recommended to be lubricated due to the direct contact between rotor [22].

Nevertheless, there are some drawbacks when applying this type of expanders. They exhibit, in general, medium levels of noise [22], which is not recommended for domestic applications. Additionally, this type of expanders are adopted in a power range higher than the scroll or piston expander due to high manufacturing costs [25]. According to Zywica, et al. [24] it is extremely difficult to buy a small screw expander with electrical capacity lower than 10 kW due to the lack of serially manufactured devices of this type.

They can be applied in systems with power outputs from 5 kW to 50 kW [22].

2.1.3. Piston Expander

In the piston expander, the working fluid enters when the piston is around the top dead centre and the inlet valve is then closed. The fluid expands as the piston is pushed by the internal pressure. The energy is transferred to the central crankshaft by connecting rod. The exit valve is opened at bottom dead centre and expanded working fluid starts moving out of the chamber as the piston moves back to the top [26]. A schematic representation of this process is shown in Figure 10.

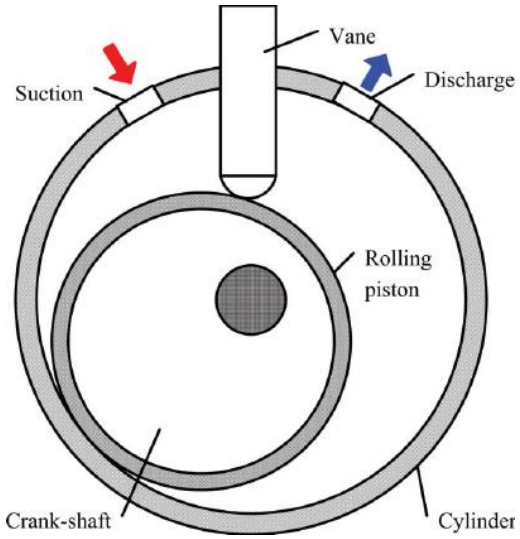

Figure 10 - Schematic representation of a piston rotary expander and its main components.

Piston expanders can be divided into several groups which differ fundamentally from each other [24,27]:

- Reciprocating piston – This kind of expander are dependable near constant volumetric rate, variable pressure capability and can be used as primary and booster compressors. Its main drawbacks are: inability to self-regulate its capacity against a given output pressure, and the size of the compressor is very large for a given capacity.
- Rotary piston expanders (Wankel rotary engines) - In general, this type of expanders presents low potential for achieving high efficiencies. Their best qualities are: small overall dimensions, low vibrations and quiet operation.
- Gerator expanders - In this case the friction between elements is not as strong as in the case of sliding friction: reduces energy losses, avoids the need of additional lubrication. Qualities: simple design, low production costs, efficiency around 85% (laboratory conditions). They have potential to become viable alternatives to other types of expanders.
- Rolling/swing piston expanders - They present low production costs, simple design. Main drawback: strong friction between a piston and a sealing vane and difficulties with providing appropriate leak tightness. Also, isentropic efficiencies do not exceed 45%.

In conclusion, piston expanders can be applied in ORC systems. This has not yet become common practice among engineers due to several factors such as: a complex construction which is directly related to their high production costs, noisy operation, high vibration levels, high friction losses, necessity to use a lubricant, and low isentropic efficiency in relation to other expansion devices [26, 22, 24].

2.1.4. Scroll Expander

A scroll expander consists of two spirals: an orbiting and fixed scroll. The orbiting scroll moves along with the fixed scroll within tight tolerances. The working fluid moves in from the centre and moves outwards inside the chamber between the orbiting and moving

scroll [22]. A schematic representation of the expander and the expansion process is shown in Figure 11.

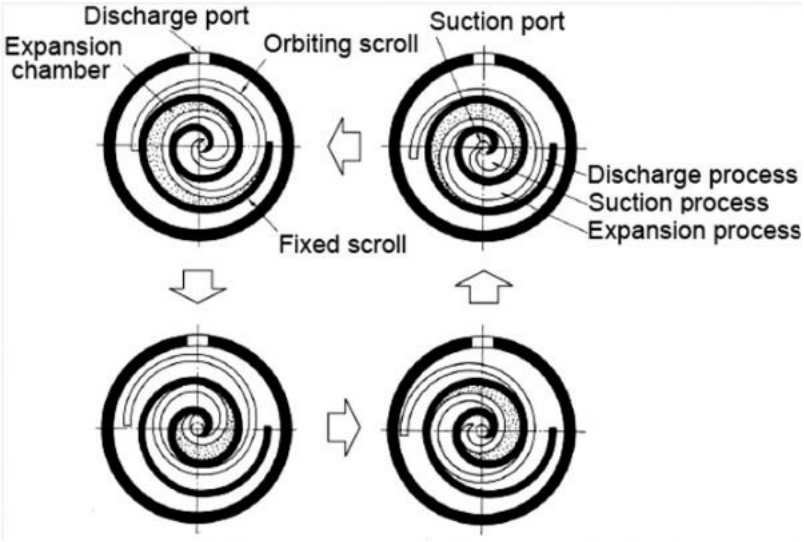

Figure 11 – Schematic representation of scroll expander's operation [22].

The scroll expander can be categorized in three different groups according to its lubrication and casing:

- Hermetic-type: the scroll coils and the attached generator are sealed in a single casing along with the compressor/expander. The working fluids may come in contact with electric coils and help to cool down the electrical systems. The machine is not supposed to be opened for services.
- Semi-hermetic: allows the machine to be dismantled for servicing and open-drive systems have generators/motors separate from the expander/compressor. The generator/motor is connected to the expansion machine by a belt or magnetic coupling allowing the sealing to be limited to expansion machine components only. One of the ways to increase the built-in volume ratio is by utilizing variable thickness walls. However, this option is still not available commercially yet.
- Oil-free machines can be used, but generally show lower volumetric performance and higher leakages due to larger tolerances between the moving parts.

The main advantages of the scroll expander are its outstanding high and stable isentropic efficiencies, exceeding 80% at different operation conditions [24]. Apart from its

simplicity and low number of components, it is compact and presents low production costs [25]. It has higher shaft speeds compared to the other volumetric machines (from 1000 to 4500 rpm) [24] and has low power outputs (lower than 10 kW_e) which is the desirable value for household's applications [22].

The major difficulty about making a scroll compressor operate in reverse as expander lies in developing an efficient bearing lubrication system, mating spiral components, and removing check valves from the compressor casing [24].

2.2. Comparison of the different expander types

In the preview subchapters were presented the expanders operations, its advantages and disadvantages for a domestic application. In this section a SWOT analysis is made for each type of expander, standing out the strengths, weaknesses, opportunities and threats, resuming the analyse that was made based on the characteristics already presented.

Table 3 - SWOT analysis of the rotary vane.

Strengths	- Direct connection to the generator (low rotational speeds;	**Weaknesses**	
-Simplicity;		- Low isentropic efficiencies;	- Leakages and higher friction losses;
-Compactness;		- Friction may increase the risk of overheating;	- Low rotational speeds (<1000 rpm).
-Reliable structure;	- Low production costs		
-Market availability;	-Small vibrations.		
Opportunities		**Threats**	
- For low temperature applications; - Suitable for power outputs below 1.5 kW_e.		-If a very high fluid temperature, the expansion of the vanes might cause them to stick and the machine will cease its operation.	

Table 4 - SWOT analysis of screw expander.

Strengths	- Compactness;	**Weaknesses**	
-Capable of gas and wet expansions;	- Higher rotational speeds (< 2000 rpm);	- Medium level of noise;	- Leakages and higher friction losses;
-Good isentropic efficiencies;	-Small vibrations.	-High manufacturing costs;	- Low rotational speeds (<1000 rpm).
Opportunities		**Threats**	
- More suitable for power outputs for the range of 5-50 kW_e.		- difficult to buy a small screw expander for small-scale (10 kW) due to the lack of serially manufactured devices of this type.	

Table 5 - SWOT analysis of piston expander.

Strengths -Simple design; -Low vibrations and quiet operation;	-Low production costs; -Small overall dimensions.	**Weaknesses** -Low potential for achieving high efficiencies;	-complex construction -Friction between a piston and sealing vane;
Opportunities - More suitable for power outputs for the range of 5-50 kW_e; -Potential to become a viable alternative to other types of expanders.		**Threats** -Still not a viable option due to better alternatives in the market.	

Table 6 - SWOT analysis of a Scroll expander.

Strengths -High isentropic efficiencies; -Simple operation; -Compactness;	-High shaft speeds (1000 to 3000 rpm) -Small number of components; -Low production costs	**Weaknesses** -The physical conversion process from a compressor to an expander is difficult;	-Its need for lubrication.
Opportunities -Low power outputs – desirable for domestic applications. -In general scroll machines are suitable in the range of 1 to 5 kW_e.		**Threats** Not found.	

As observing this SWOT analysis, it is possible to conclude that the scroll expander stands out for its several strengths and low weaknesses for domestic applications compared with the other types. To compare this type of expanders more directly, the following table (see Table 7) will account each characteristic for each expander having always in mind that the objective of these expanders is for domestic application.

Table 7 - Direct comparison of the main four expanders presented.

Expander type	Compactness	Low noise and vibrations	Costs	Isentropic efficiency	High supply pressure and temperature	Max rotational speed (rpm)	Suitable Outputs (kW_e)
Rotary vane	+ +	+ +	+ +	+	-	< 1000	< 1,5
Screw	+ + +	+	-	+ +	+	< 2000	5 - 50
Piston	+	-	+ +	-	+ + +	< 4000	5 - 20
Scroll	+ +	+ +	+ +	+ + +	+ + +	< 3000	1 - 5

Although rotary vane, screw and piston have their advantages in some characteristics, the scroll expander is the one with better overall evaluation for domestic applications, and therefore, the chosen one for this study. From the different types of casing, the hermetic casing is the one that suits best due to its compactness and has the generator integrated. Thus, the final choice is the hermetic-scroll expander. The major difficulty associated with the use of this positive displacement machine is its lubrication. This topic will be developed further on.

3. IMPLEMENTATION OF A MICRO-SCALE EXPANDER IN THE EXISTANT TEST BENCH

3.1. Description and analysis

As mentioned in the Introduction section, the Mechanical Engineering Department of the University of Coimbra developed a test bench with the objective to study micro-CHP based on ORC. The existent test bench was built, primarily, to study the evaporator, one of the most important components of this ORC system. Besides the evaporator, the main components of this cycle are: a pump, an expansion valve, and a condenser. A schematic diagram of this system is presented in Figure 12. The cycle starts with the organic fluid (Genetron R245fa) being pressurized in the pump (Fluid-o-Tech TMFR series) after which is directed to the evaporator (design and manufacture as presented in [28]) where is heated, vaporized and superheated by the combustion gases generated in a natural-gas burner (BurnerTech VAPAC 40). Later, the pressurized vapor flows through a needle throttling valve (ValSteam PRC25I) where it is expanded. The low-pressure vapour is conducted to a braze plate heat-exchanger (GEA WTT GBS220H) where the heat transfer causes the condensation of the fluid. To close the cycle, the fluid is then driven to the pump, to be pressurized again. This specific test bench uses a new type of evaporators that contains a double heat exchanger in its inside. The first one (referred as water post-heating section in Figure 12, and as PH along this work) is placed between the heat source (a natural gas burner) and the second heat exchanger (referred as working fluid heating section in Figure 12, and as EHE along this work) and has a double objective: i) reduce the combustion gases temperature before they reach the EHE and ii) complete the heating process of the CHP water that started in the ORC-condenser. This second objective will increase the ORC electrical efficiency by decreasing the average temperature in the condenser which can promote a higher expansion process in the expander. This arrangement, using this new type of evaporators, has been denominated in the literature as a CHP hybrid configuration.

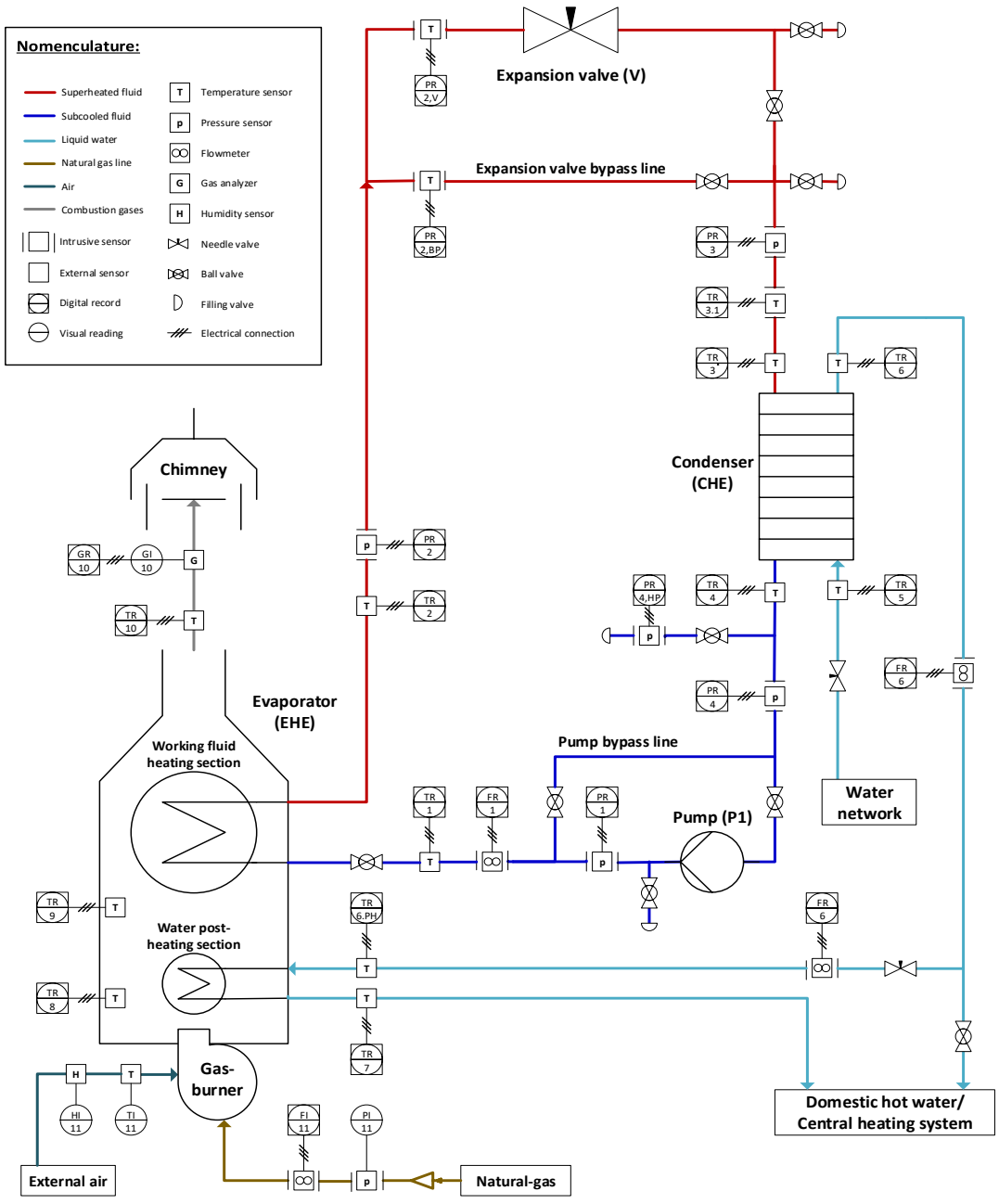

Figure 12 - Schematic diagram of the existent test bench in DEM-UC.

Once this installation was created to study the evaporator, a needle throttling valve was implemented instead of a real expander. Introducing that component in the ORC will convert the test bench into an actual CHP unit, enabling new and state-of-the-art studies

which can lead to the breakthrough of residential CHP systems based on ORC technology. Therefore, it is the main objective of this work.

As already mentioned in section 2.1.4, for the expander's proper functioning it is necessary to include a lubrication system. Therefore, it is relevant to evaluate the impact of this requirement over the ORC. Opposite to this lubrication system, the electrical connections of the expander, that includes the electrical energy dissipation and its control, will not be evaluated throughout this work.

3.2. Expander selection methodology

After the description and analysis of the existent test bench, the implementation of the adequate expander and its lubrication system is assessed. The selection of the expander within the ORC will be firstly made without considering any aspect about the lubrication. This is made because: i) it is not expected a significant influence in the operation of the system (due to low oil ratios values that are usually defined) and ii) the inclusion of oil within the fluid flow will only change the transport proprieties and not the selection methodology.

3.2.1. Selection methodology

As concluded in section 2.2, the most suitable expander technology for the residential scale (1-5 kW_e) is the scroll type with a hermetic housing. It is essential to mention that this technology is already available in the market, however, it presents high acquisition costs. Considering this, low-cost solutions, like HVAC compressors, should be studied and converted to work as an expander for this application. To select the suitable expander, it is necessary to build a physical model in order to understand its thermodynamic behaviour. Apart from the detailed expander model, a simplified one is made for the ORC to evaluate the influence of adding a real expander to the cycle. However, as previously mentioned, these models will be developed neglecting the expander lubrication at a first instance. Both of the models are developed using Matlab® software with the REFPROP thermodynamic database [29].

3.2.1.1. ORC Model

Before the development of the expander model, the operating conditions and interaction between the main components of the ORC must be defined. To do so, a simplified ORC model, based on the study made by Pereira *et al*. [30], is established. This model considers no heat or pressure losses in the connecting pipes and neglects the electromechanical inefficiency of the pump. The input parameters of this model are listed in Table 8 and were retrieved from the above mentioned study ([30]). These inputs represent the design operating conditions of the system. The numeration used in the symbology of Table 8 corresponds to the schematic diagram shown in Figure 12.

Table 8 - Input parameters of the ORC model.

Inputs	Symbol	Value
CHP water inlet temperature	T_5 [ºC]	10
CHP water outlet temperature	T_7 [ºC]	65
Water post heating fraction	θ [%]	22 [1)]
End-user thermal power demand	Q_w [kW]	25
Working fluid	-	R245fa
Maximum ORC pressure	p_{max} [kPa]	1200
Super heating degree of the fluid	ΔT_2 [ºC]	10
Pump isentropic efficiency	η_P [%]	50
Condenser efficiency	η_{CHE} [%]	98
Evaporator efficiency	η_{EHE} [%]	90

[1)] Most demanding condition for the ORC net power output according to the results presented in [30].

Within the list observed is the water post-heating fraction (θ) that can be defined as the fraction of the water heating process that is done in the PH section of the ORC evaporator. For instance, for a value of θ = 0% refers to a standard CHP system in which all the water heating process occurs in the ORC-condenser, while a value of θ = 100% states a situation which the ORC is not working. The value of θ is defined by the equation (3.1).

$$\theta = \frac{T_7 - T_6}{T_7 - T_5} \times 100 \tag{3.1}$$

To avoid problems related with the pinch-point in the ORC-condenser, the model assumes that the condensing temperature is limited (inferiorly) by the water temperature at the ORC-condenser exit. The energy balance equations, presented in Table 9, can be solved with the values of the enthalpy in their respective key points.

Table 9 - Power balance equations for each ORC component.

Components	Fluid	Power balance
Condenser	Water	$\dot{Q}_{CHE,w} = \dot{m}_w \times (h_6 - h_5)$
	R245fa	$\dot{Q}_{CHE} = \dot{Q}_{CHE,w}/\eta_{CHE}$
Evaporator – PH	Water	$\dot{Q}_{PH} = \dot{m}_w \times (h_7 - h_6)$
Evaporator – EHE	R245fa	$\dot{Q}_{EHE} = \dot{m} \times (h_2 - h_1)$
Pump	R245fa	$\dot{W}_{in} = \dot{m} \cdot (h_1 - h_4)$
Hybrid CHP system	Water	$\dot{Q}_w = \dot{m}_w \times (h_7 - h_5)$
	R245fa	$\dot{Q}_{CHE} = \dot{m} \times (h_3 - h_4)$

However, as can be observed in Table 8 and Table 9, there is no information about the expander (such as isentropic efficiency, mass flow rate, and others). It was intentional because the selection of the expander, demands for a development of a detailed semi-empirical model (described in the next section) that will establish those missing aspects in the global ORC model.

3.2.1.2. Expander Model

The semi-empirical model of the scroll expander was developed based on the proposals made by Lemort *et al.* [31,32] and Giuffrida *et al.* [33]. The methodology presented in both papers is developed for scroll type expanders integrated in micro-scale ORC. The conceptual scheme of the expander model is shown in Figure 13 and is resumed along this section. In this figure, the supply section (*su*) corresponds to the local identified with the index 2 in Figure 12 as well as the outlet (*ex*) will correspond to the local identified with the index 3. The variables must be then, accordingly adapted.

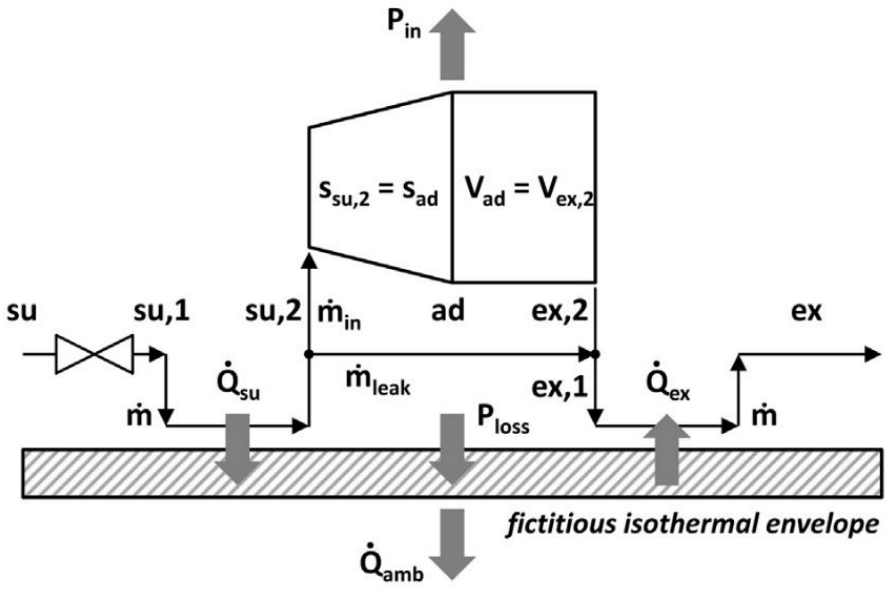

Figure 13-Conceptual scheme of the expander model proposed by Lemort *et al.* [31]

The evolution of the fluid through the expander, as presented in Figure 13, is decomposed into the following successive steps (the nomenclature used in Figure 13 will support the description then presented):

i. Adiabatic supply pressure drop (process from *su* to *su,1*):

This process considers all the pressure losses between the expander inlet and the variable volume chamber. It is simulated as an isentropic flow through a converging nozzle whose cross-sectional area is A_{su}. (stands for an average value of the inlet port effective area over the entire supply process). The mass flow rate entering the expander ($\dot{m}$) can be calculated as shown in equation (3.2). This equation represents a combination of the equations of mass and energy conservation through a nozzle.

$$\dot{m} = \rho_{su,1} \times A_{su} \cdot \sqrt{2 \times (h_{su} - h_{su,1})} \tag{3.2}$$

Besides the variables already mentioned, $\rho_{su,1}$ and $h_{su,1}$ refer to the density and enthalpy of the fluid after the pressure drop respectively, and the variable h_{su} is the enthalpy at the inlet of the expander.

ii. Isobaric supply cooling down. (process from *su,1* to *su,2*):

The cooling down process occurs due to the contact with the metal mass of the machine. The main heat transfer mechanisms inside the scroll expander occur between:

- The expander shell and the fluid in the supply and exhaust pipes;
- The scrolls (fixed and orbiting) and the fluid in the suction, expansion and discharge chambers;
- The expander shell and the ambient.

In order to have a more accurate calculation of the heat transfers in the supply and exhaust area, it is considered a fictious metal envelope of uniform temperature (T_w). This fictitious envelope represents the metal mass associated to the expander shell. Then, the supply heat transfer loss ($\dot{Q}_{su}$) is given by equation (3.3), where AU_{su} represents the supply heat transfer coefficient, $h_{su,2}$ symbolizes the enthalpy of the fluid that enters in the casing, c_p the Specific heat of the fluid, and $T_{su,1}$ the temperature of the fluid after the cooling down. and T_w.

$$\dot{Q}_{su} = \dot{m}\left(h_{su,1} - h_{su,2}\right) = \left[1 - e^{-\frac{AU_{su}}{\dot{m}\cdot c_p}}\right] \times \dot{m} \times c_p \times (T_{su,1} - T_w) \tag{3.3}$$

The value of AU_{su} depends on the mass flow rate, as presented in Equation (3.4), where $AU_{su,n}$ is the nominal supply heat transfer coefficient corresponding to the nominal mass flow rate.

$$AU_{su} = AU_{su,n} \times \left(\frac{\dot{m}}{\dot{m}_n}\right)^{0,8} \tag{3.4}$$

iii. Internal leakage (processes from *su,2* to *ex,2*):

As observable in Figure 13, the mass flow rate entering the expander is split into two parts: one causes the rotation of the shaft at a specified rotational speed while the other part is leaked (not expanded).

There are two ways of leakage in a scroll expander: i) the gaps between the bottom or the top plate and the scrolls (denominated as radial leakage), and ii) a flank leakage

results from a gap between the flanks and the scrolls. However, in this model, it is considered only one fictitious leakage which combines all the mentioned leakages. With this, it is relevant to identify the hypothetical cross-sectional area of the leakage's paths (A_{leak}), the flow rate of the leakage ($\dot{m}_{leak}$), and the leakage throat pressure (p_{leak}). The p_{leak} is equivalent to the maximum value between the exhaust pressure ($p_{ex,2}$) and the leakage critical pressure ($p_{crit,leak}$). The value of $p_{crit,leak}$, can be obtained by equation (3.5) that considers the working fluid as an ideal gas. In this equation, $p_{su,2}$ refers to the inlet pressure of this nozzle (pressure of the fluid after the pressure drop at the entrance of the expander) and γ is an isentropic exponent which assumes the value of 1,1.

$$p_{crit,leak} = p_{su,2} \times \left[\left(\frac{2}{\gamma+1}\right)^{\left(\frac{\gamma}{\gamma-1}\right)}\right] \tag{3.5}$$

To complete the characterization of the leakages, it is necessary to define its flow rate ($\dot{m}_{leak}$) which, as made by the equation (3.6) that similar to the calculation made for the supply pressure drop section, express the combination of the mass and energy conservation equations through the nozzle. In this equation, the density (ρ_{leak}) and its enthalpy (h_{leak}) are calculated considering the maximum value between $p_{ex,2}$ (pressure at the outlet of the expander) and $p_{crit,leak}$ and an isentropic condition ($s_{leak} = s_{su,2}$).

$$\dot{m}_{leak} = \rho_{leak} \times A_{leak} \times \sqrt{2 \times (h_{su,2} - h_{leak})} \tag{3.6}$$

iv. Isentropic expansion (processes from *su,2* to *ad)*:

This expansion was adapted to the pressure imposed by the built-in volume ratio ($r_{v,in}$) of the machine. With the $r_{v,in}$ and the density correspondent to the fluid at the inlet of the scroll ($\rho_{su,2}$) it is possible to achieve the value of the specific volume after the expansion (v_{ad}) and the respective density (ρ_{ad}) as shown in the equations (3.7) and (3.8).

$$v_{ad} = \frac{r_{v,in}}{\rho_{su,2}} \tag{3.7}$$

$$\rho_{ad} = \frac{1}{v_{ad}} \tag{3.8}$$

As can be concluded from the observation of the Figure 13, the total mass flow rate that enters in the expander ($\dot{m}$) is the summation of the internal mass flow rate ($\dot{m}_{in}$) and leakage mass flow rate ($\dot{m}_{leak}$). This is represented in the equation (3.9)

$$\dot{m} = \dot{m}_{in} + \dot{m}_{leak} \tag{3.9}$$

The $\dot{m}_{in}$ can be expressed as the quotient between the volume flow rate ($\dot{V}_{s,exp}$) and the specific volume of the fluid ($v_{su,2}$) after the initial pressure drop and cooling down process. This is presented in the equation (3.10).

$$\dot{m}_{in} = \frac{\dot{V}_{s,exp}}{v_{su,2}} = \frac{N \times V_{s,exp}}{v_{su,2}} = \rho_{su,2} \times \frac{V_{s,exp}}{r_{v,in}} \times \frac{N}{60} \tag{3.10}$$

In this equation the $\dot{V}_{s,exp}$ corresponds to the multiplication of the swept volume of the expander ($V_{s,exp}$) and its rotational speed (N). These parameters are both inputs of the model. Finally, $v_{su,2}$ can be substituted by the relation between $\rho_{su,2}$ and $r_{v,in}$.

v. Adiabatic expansion at a constant volume (processes from *ad* to *ex,2*):
At this stage an under- or an over-expansion of the fluid may occur (represented in Figure 14). Under-expansion happens when the internal pressure ratio ($p_{su,2}/p_{ad}$), imposed by expander is lower than the system pressure ratio ($p_{su,2}/p_{ex,2}$). This means that the pressure at the end of the process, in the expansion chambers, is higher than the discharge line. To match these pressures, it is assumed that some fluid flows out of the discharge chambers. The opposite process occurs for an over-expansion

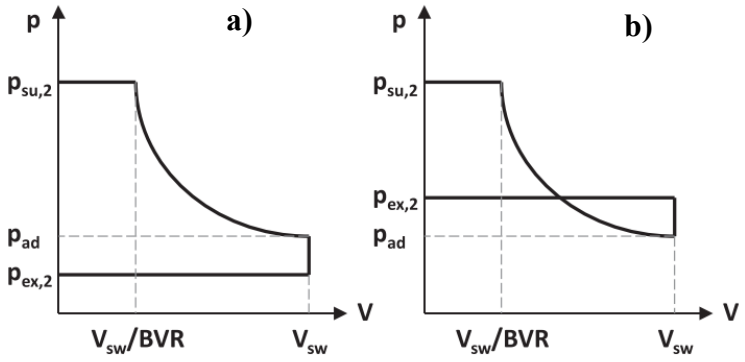

Figure 14 - Schematic under- and over-expansion processes in the p-V diagram (on the left and on the right, respectively).

vi. Adiabatic fluid mixing (processes from *ex, 2* to *ex,1*):
When the mass flow rate related to shaft rotation ($\dot{m}_{in}$) meets the leakage flow rate ($\dot{m}_{leak}$), results in a slight increase in specific enthalpy. In this model it was considered a weighted average of these enthalpies as represented in Equation (3.11).

$$h_{ex,1} = \frac{\dot{m}_{in} \times h_{ex,2} + \dot{m}_{leak} \times h_{su,2}}{\dot{m}} \tag{3.11}$$

vii. Isobaric exhaust heating-up or cooling down (processes from *ex,1* to *ex*):
In an analogous way to step ii), a heat exchange between the fictious isothermal envelope and the fluid occurs. Therefore the calculation methodology used is similar to the equation (3.3), as shown in equation (3.12).

$$\dot{Q}_{ex} = \dot{m}\left(h_{ex,1} - h_{ex}\right) = \left[1 - e^{-\frac{AU_{su}}{\dot{m}\cdot c_{p,ex1}}}\right] \times \dot{m} \times c_{p,ex,1} \times (T_{ex,1} - T_w) \tag{3.12}$$

After establishing the thermodynamic processes within the expander, it is possible to calculate several performance parameters like the power generated by the expander (P_{in}), or the shaft power (P_{sh}) through the equations (3.13) and (3.14) respectively.

$$P_{in} = \dot{m}_{in}\left[\left(h_{su,2} - h_{ad}\right) + v_{ad} \times \left(p_{ad} - p_{ex,2}\right)\right] \tag{3.13}$$

$$P_{sh} = P_{in} - P_{loss} \tag{3.14}$$

The mechanical losses (P_{loss}), that are caused by the friction between the scrolls and losses in the bearings, can be calculated by equation (3.15), where τ_{loss} represents the mechanical loss torque (which is a characteristic of the selected expander and so an input of the model).

$$P_{loss} = \frac{2 \times \pi \times N}{60} \times \tau_{loss} \tag{3.15}$$

In this model it is assumed that the electromechanical efficiency is equal to 95%. With this, the electrical power output ($\dot{W}_{out}$) of the expander can be estimated as shown in equation (3.16).

$$\dot{W}_{out} = P_{sh} \times 0{,}95 \tag{3.16}$$

The isentropic efficiency can be expressed as stated in equation (3.17), where $h_{ex,i}$ represents the outlet enthalpy as the process was isentropic *(*$s_{su} = s_{ex}$*)*

$$\eta_i = \frac{P_{in}}{\dot{m}\left(h_{su} - h_{ex,i}\right)} \tag{3.17}$$

Another relevant efficiency to consider is the mechanical efficiency (η_m) and it is estimated as exposed in equation (3.18).

$$\eta_m = \frac{P_{sh}}{P_{in}} \tag{3.18}$$

The global efficiency (η_g) is a relation between the η_m and η_i and is calculated as presented in equation (3.19).

$$\eta_g = \eta_m \times \eta_i \tag{3.19}$$

Regarding the total heat losses to the ambient ($\dot{Q}_{amb}$), it can be calculated from equation (3.20) where AU_{amb} represents a global heat transfer coefficient between the housing and the ambient.

$$\dot{Q}_{amb} = AU_{amb} + (T_w - T_{amb}) = P_{loss} + \dot{Q}_{su} + \dot{Q}_{ex} \tag{3.20}$$

This semi-empirical model is solved by an iterative process since some initial values of some parameters, needed to evaluate the transport proprieties, are unknown (e.g.: T_w or $T_{su,1}$). In order to resume the expander model, a simplified flow chart showing the necessary inputs and expander's parameters as well as its main outputs, presented in Figure 15.

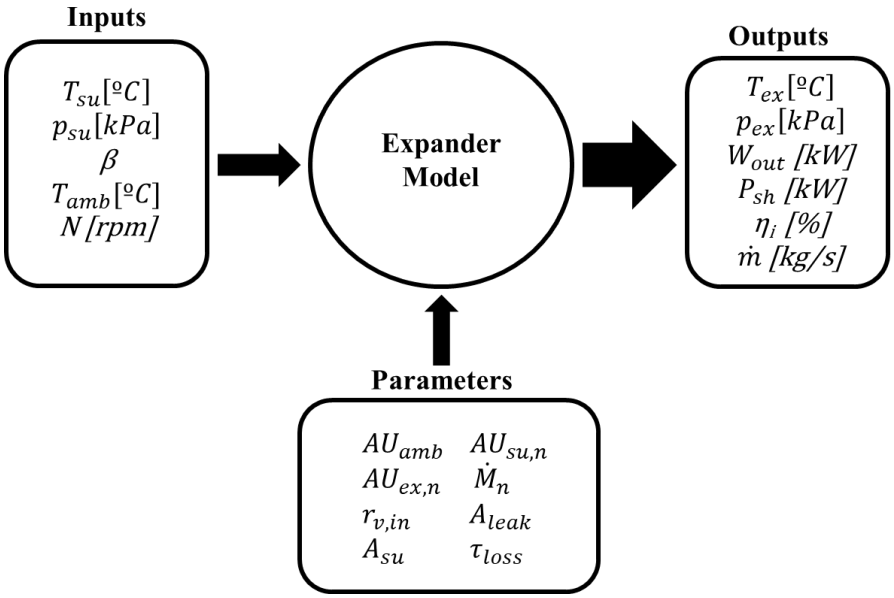

Figure 15 - Flow diagram of the expander model.

After analysing Figure 15, to run this model, the expander should be selected once some inputs regarding its physical parameters are needed. It is important to remember that a compressor will be converted to work as an expander in this work. Therefore, a deeply research in the market was made regarding the main manufactures and the power size (micro-scale). From this, the hermetic compressor ZR61KRE-TFD from the company Copeland emerged (technical sheet available in Annex 1). This type of compressors (not this specific model) has already been converted with success to work as an expander in [11,34]. Besides that, it presents a small size and an average power ranging from 2,8 to 2,9 kW (operating as compressor in its nominal condition) which is frame for domestic applications. A photograph of the compressor, together with a detailed drawing and its main (available) characteristics are presented in .

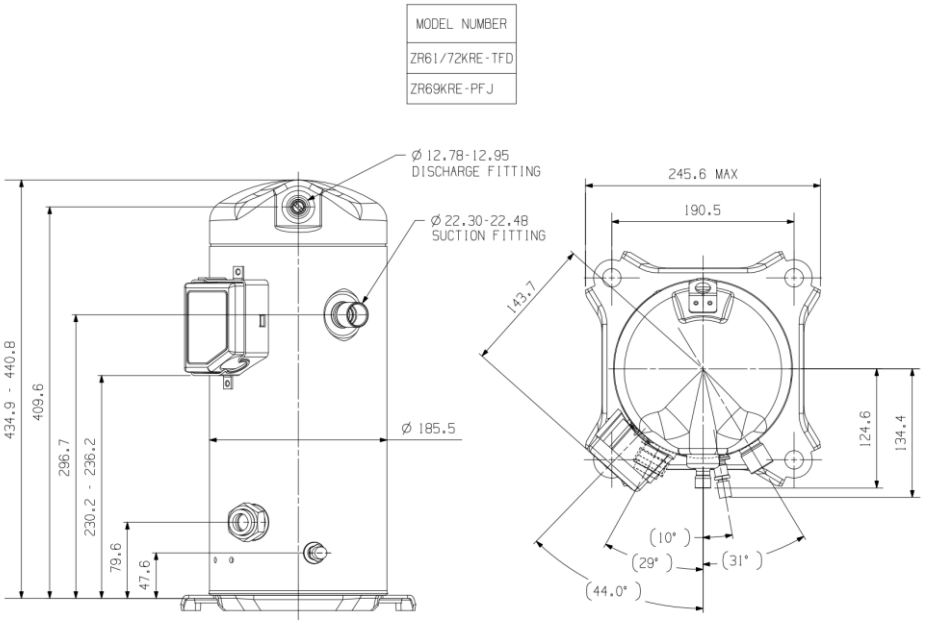

Displacement, ($\dot{V}$) m^3/h	14,4
Oil Quantity, l	1,9
Oil type	POE RL32-3MAF
Rotational speed (N), rpm	2900

Figure 16 – Technical data and photography of the compressor ZR61KRE-TFD.

After the analysis of the table presented in Figure 16, it can be concluded that most of the necessary parameters to run the model are not provided by its manufacturer. One of those is the swept volume, ($V_{s,exp}$). However, this specific parameter can be obtained from the relation between the displacement ($\dot{V}$) and the rotational speed (N), as shown in the equation (3.21).

$$V_{s,exp} = \frac{\dot{V}}{N \times 60} \tag{3.21}$$

The swept volume is one of the most important and relevant parameters to characterize these types of components. Therefore, and once there is still several variables not provided by the manufacturer, a methodology to its identification was created. That consists in establishing a relation between the swept volume of the compressor and the desirable unknown variable (a characteristic of the compressor). This relation entails an interpolation, regarding the swept volume and the unknown variable, between two different size compressors and the selected one (which has the unknown variable). The identification of those unknown variables and the results obtained for the compressor ZR61KRE-TFD using this methodology, are presented in the Table 10.

Table 10 - Identified parameters of the expander model.

Ambient heat transfer coefficient	$\boldsymbol{AU_{amb}}$	3,58 W/K
Supply heat transfer coefficient	$AU_{su,n}$	11,86 W/K
Exhaust heat transfer coefficient	$AU_{ex,n}$	19,13 W/K
Nominal mass flow rate	$\dot{m}_n$	0,0671 kg/s
Leakage area	A_{leak}	4,9 mm^2
Supply cross sectional area	A_{su}	19,94 mm^2
Mechanical loss torque	τ_{loss}	0,2628 N.m

Additionally to the identification of the variables presented in Table 10 the built-in-volume ratio ($r_{v,in}$) was still not identified. For this, it was necessary to develop another methodology based on the software Select8®. This software is provided by the compressor manufacturer (Copeland) and has the capacity to simulate its use in several different operating conditions. Although this software cannot identify directly the missing variable, the operating conditions given were used in the expander semi-empirical model to create a new iterative process in order to match those conditions by changing the built-in volume ratio value. This process was executed for different operational conditions, and the volume ratio used in the model was the average of these results. It is important to mention that the difference between the values obtained was not significant. As a conclusion, the built-in volume ratio for this compressor is, approximately, 3,27.

3.2.2. Lubrication system

After the definition of the expander, the lubrication system, which is essential to ensure its efficient operation, must be designed.

For this question, two main hypotheses were found in the literature:

i. The oil flows through the complete ORC system, mixing with the organic fluid [11,18,21,35];
ii. The oil only circulates in the expander section. In this hypothesis, an oil separator is placed after the expander, where the oil will be separated from the working fluid and pumped again to the entrance of the expander [10,13].

Within the existing test benches in the literature, it was concluded that a significant part presented the solution where the mixture of the fluid and the oil flows in the complete cycle. The primary justifications for this choice are based on economical and simplicity reasons [36]. Avoiding oil circulation requires other components, such as an oil separator, an oil pump, a heat exchanger and an oil tank, impacting the costs and the system's compactness. However, several authors refer that the oil-fluid mixture impacts the overall system's efficiencies [11,35]. Once the solution is not clear, a deeper research was made in order to understand the impact of the lubrication in the cycle.

Suppose it was considered the first hypothesis, with the lubricant oil flowing through the ORC, the mixture becomes approximately a zeotropic fluid when a liquid phase is present. Here, the thermodynamic proprieties are considered similar to the pure refrigerant due to the relatively low fraction of the lubricant compared to the refrigerant. However, when the fluid is at a two-phase or vapor condition, the situation becomes different. Here, the mixture is always in a two-phase condition due to the considerably high boiling point of the oil. As a vapour quality increases, the impact of the oil entrainment on the fluid enthalpy is substantial, and the calculated mixture enthalpy is lower than the pure refrigerant [37].

The impact of the oil is often neglected by the scientific community, but it can result in a complete misunderstanding of the system's performance [38]. Moradi *et al*., Feng *et al*., and Dickes *et al*. [36–38] developed experimental studies in order to determine each component's impact. A resume of those conclusions is presented in order to assess what is the best option for this test bench.

The pump power consumption and the consequent BWR (Back Work Ratio) vary with lubricant oil ratio at different superheating degrees. BWR is denoted by the ratio between pump consumption and the expander output. The pump power consumption and BWR have a similar decreasing trend with the increase of the lubricant oil ratio. This increment in lubricant oil ratio ensures the decline in pump outlet pressure, resulting in the decrease in pump enthalpy drop, enabling the decrease in pump power consumption [36].

When referring to the heat exchangers, the lubricant oil impacts more the condenser performance than the evaporator [37]. Their convection modes can explain it: in the evaporator the bubbling mixes the lubricant oil, reducing the thermal resistance due to the oil film on the heat exchange surface; in the condenser, the oil forms a film on the heat exchange surface. In addition to this, according to Moradi, *et al*.[37], the lubricant impacts the evaporator performance more severely in higher super-heating degrees. For the evaporator, it is crucial to consider the risk of oil accumulation, and hotspots [23]. This aspect is pertinent for this study as the present test bench has direct vaporization. As mentioned in the Introduction chapter, with direct vaporization is more difficult to control the temperature surface of the evaporator. This statement, allied with the risk of hotspots, can be dangerous.

The impact of the lubricant on the expander also cannot be ignored. The mixture passing through improves the sealing factor [38] and thus reduces internal leakages at higher shaft speeds. The mechanical efficiency is reduced, and for the same shaft power, the thermal power of the expander is increased and consequently, the mechanical efficiency decreases [39]. As shown in Figure 17, there is a slight increase in the isentropic efficiency while there is a decrease in shaft power with the increase of the oil ratio. In this figure, the isentropic efficiency is higher than 100%, for higher oil ration with superheating degree of 5ºC, which is not realistic. The authors state that there is an experimental measuring error because a significant part of the mixture (oil and fluid) founds itself at a two-phase condition.
[36].

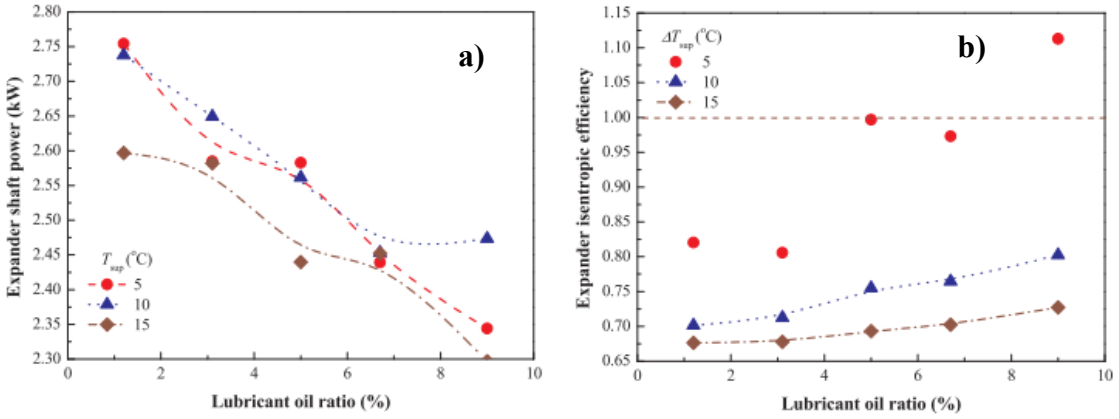

Figure 17 – Influence of the lubricant oil ration, for different superheating degrees, over a) shaft power and b) isentropic efficiency [36]**.**

Summing up this analysis, the lubricant oil influences the pump operation since it decreases gradually the pump power consumption. On the other side, it deteriorates the expander shaft power and thus electrical power. The isentropic efficiency and the sealing factor increase and there is a reduction on internal leakages. In the evaporator and in the condenser, the heat transfer coefficient diminishes with the lubricant oil ratio due to the fouling factor (oil film) created. According to Feng, *et al*. [36], it can be concluded the lubricant oil reduces the system generating efficiency.

In conclusion, the lubricating factor cannot be neglected in this system. With the statements previously presented, the mixture of the lubricating oil and working fluid circulating in the system is not beneficial, adding the fact of the risks associated with the creation of hotspots. As the lubrication is essential for the proper functioning of the expander, it is considered that the option ii), i.e., the implementation of an external oil system is the best choice for this work. Besides, it is also important to mention that this analysis neglects any restraint regarding the cost of reproducing any of these solutions. However, and in spite of not being selected, it is predicted that this solution with the mixture of oil and fluid circulation in the system has a reduced acquisition/installation cost.

Therefore, to implement this solution, the oil should be introduced into the piping before the expander and removed after the expansion by an oil separator, preventing it from going to any heat exchanger section. To do this, an external oil circulation system should be implemented as schematically represented in Figure 18.

In addition to the oil separator after the expander, this oil circuit demands two more important components: i) pump and ii) a heater. The pump is justified by the need of controlling the mass flow rate (and so the oil percentage within the expander), and to deal with the hydraulic pressure losses (and the different pressures before and after the expander). On the other hand, the oil heater is necessary to avoid the condensation of the fluid at the entrance of the expander due to the low temperature of the oil (that comes from the outlet of the expander, with lower temperatures due to the expansion process). Other components like the oil tank or valves (presented schematically in Figure 18) are also need but just for safety/operational purposes.

When selecting the expander, one of the technical information is its oil type. As presented in Figure 16 the oil type is POE RL32-3MAF and the required quantity is 1,9 L.

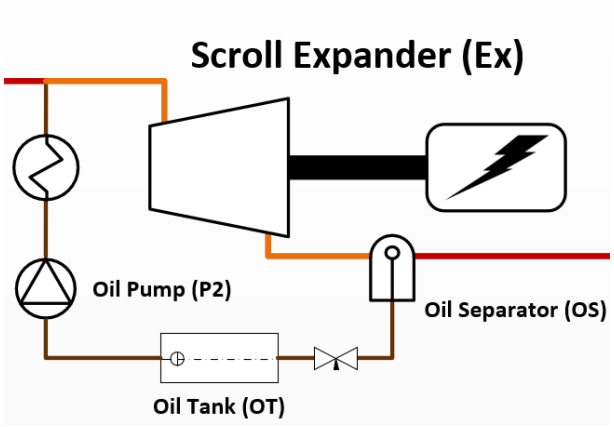

Figure 18 - Schematic representation of the oil circulation system.

After the definition of the main components, a brief research was conducted in order to find the proper suppliers.

For the oil separator, there are four main types: helical, washing, packed and filter. The recommended oil separator for this application is the helical oil separator [40]. This type of oil separator offers 99 to 100% efficiency in oil separation with low pressure drop. The operation of this oil separator is schematically represented in Figure 19. The fluid (in gas form) – oil mixture at the outlet of the expander enters in the oil separator and is centrifugally forced along the spiral path of the helix, causing heavier oil particles to spin to the perimeter

where impingement with a screen layer occurs. This screen layer serves as an oil stripping and draining medium [41].

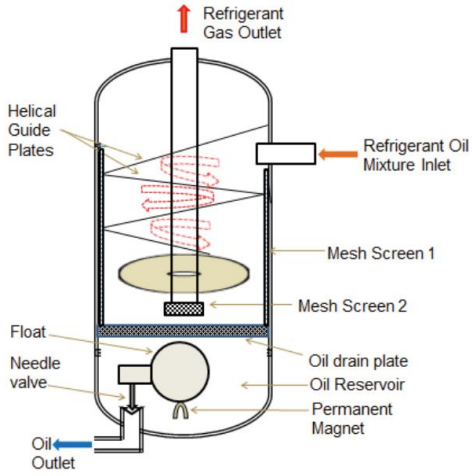

Figure 19 - Schematic representation of a helical oil separator operation.

When selecting the pump type, it is important to consider the low flow rate of the oil. With this, the positive displacement pumps are the most adequate for this application. There are 4 main candidates for this application: i) progressive cavity pump, ii) gear pump (internal and external), iii) vane pump (impeller pump) and iv) a peristaltic pump. Due to the low mass flow rate expected for the oil, a peristaltic pump can be adequate for this system. Its working principle, shown in Figure 20, is based on moving a product through a hose, by compressing and decompressing. The 'shoes' of the pump are fixed onto the rotor of the pump, which press the fluid through the pump. The temperature limit of this component is defined by the material used in the tubes. However, if Viton was considered as example, it can withstand a temperature of around 200ºC [42].

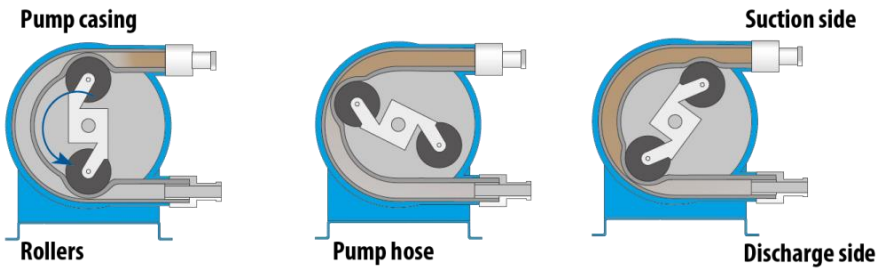

Figure 20 - Schematic representation of the working principle of a peristaltic pump.

Regarding the oil heater a simple (and easily found in the market) spiral electric resistance involving the tube is sufficient to accomplish the necessary work.

With this modification, the model of the expander was updated to consider the organic fluid (R245fa) and oil (POE RL32-3MAF) mixture to understand its consequences in the operation of the system.

In this context, the study made by Jia *et al*. [43] gives information that allows the proprieties calculations of this mixture. Based on this, the enthalpy of the mixture (h_t) can be calculated as represented in equation (3.22).

$$h_t = (1 - X - C_g) \times h_{L,r} + C_g \times h_{oil} + X \times h_{V,r} \tag{3.22}$$

Where, $h_{L,r}$ and $h_{V,r}$ are the enthalpy of the organic fluid at liquid and vapour phase, respectively, X, identifies the vapour quality (calculated by equation (3.24)), h_{oil} the enthalpy of the oil and C_g represents the oil circulating mass fraction which can be obtained as shown in equation (3.23).

$$C_g = \frac{m_{oil}}{m_{L,r} + m_{oil} + m_v} \tag{3.23}$$

$$X = \frac{m_v}{m_{L,r} + m_{oil} + m_v} \tag{3.24}$$

In equation (3.24), m_v and $m_{L,r}$ symbolise the mass flow rate of the refrigerant in vapor and liquid phase respectively and m_{oil} the mass flow rate of the oil.

It is important to consider that at the entrance of the expander the refrigerant in vapour phase only, so $m_{L,r}$ is negligible.

The specific enthalpy of the oil can be calculated by following the equation (3.25).

$$h_{oil} = h_{ref} + \int_{T_{ref}}^{T} C_{p,oil}\, dT \tag{3.25}$$

In this equation, h_{ref} represents the reference enthalpy that is 200 kJ/kg, and T_{ref} the reference temperature (that is considered 273,15 K). The specific heat capacity of the oil

($C_{p,oil}$) is calculated by Liley and Gambill correlation presented in equation (3.26), where ρ_{oil} is the density of the oil at 288,71 K.

$$C_{p,oil} = \frac{0{,}75529 + 0{,}0034 \times T}{\sqrt{\rho_{oil}/998{,}5}} \tag{3.26}$$

As can be concluded, to apply this methodology it is necessary to have the oil density along the temperature variations. The proprieties of the oil were requested to the supplier and searched in the REFPROP thermodynamic database, but no information was obtained. To this end, it was found in the literature the article by Morais *et al.* [44] where there were identified the propriety variation of this specific oil within a temperature range. This allowed the calculations of the regression curves (presented in Figure 21) and, this way, turns possible to implement.

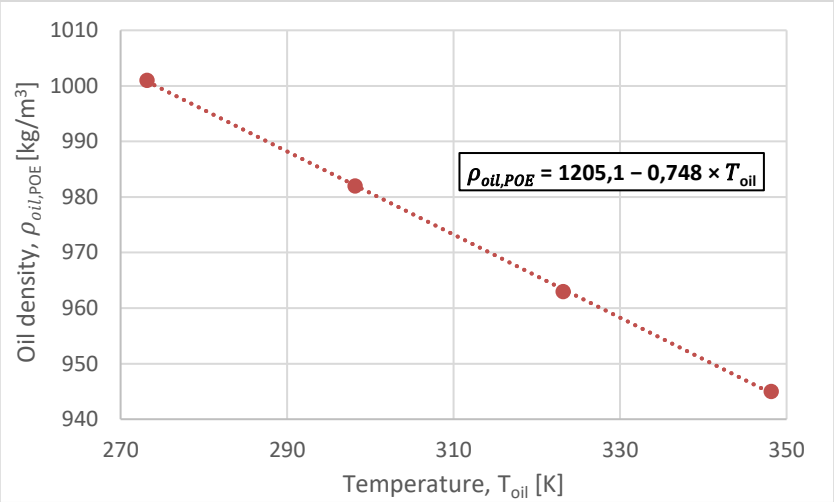

Figure 21 - Relation between the density and temperature of POE RL32-3MAF.

Regarding the density of the mixture (ρ_{mix}) it was applied a method based on Dickes *et al.* [45] and described in equation (3.27). In this equation, ζ_{wf} is the fluid fraction, $\rho_{wf,i}$ represents the density of the working fluid and K the ideal density correction factor that can be estimated based on the chart presented in Figure 22.

$$\rho_{mix} = \frac{\rho_{oil,POE}}{1 + \zeta_{wf} \times \left(\frac{\rho_{oil,POE}}{\rho_{wf}} - 1\right)} \times \frac{1}{K} \tag{3.27}$$

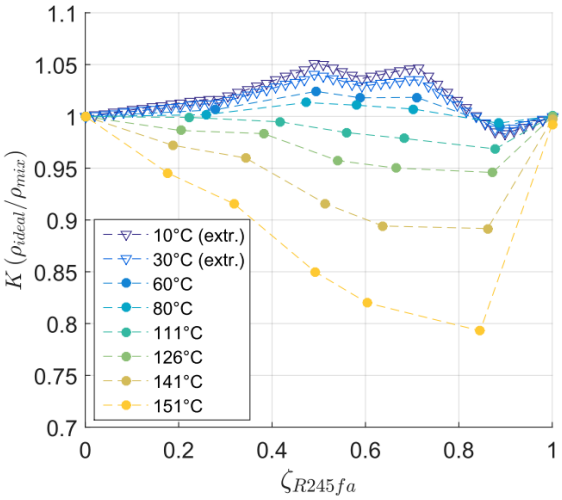

Figure 22 – Correction factor for the liquid density calculation [45]**.**

3.3. Results and parametrical analysis

In order to understand the influence of certain parameters in the behaviour of the system, a parametrical analysis was conducted where the values of the electrical energy output and the efficiencies are taken for different values of oil fraction. Besides the value of the oil fraction, the inputs applied are the ones presented in Table 8 The results are shown in Figure 23 and Figure 24.

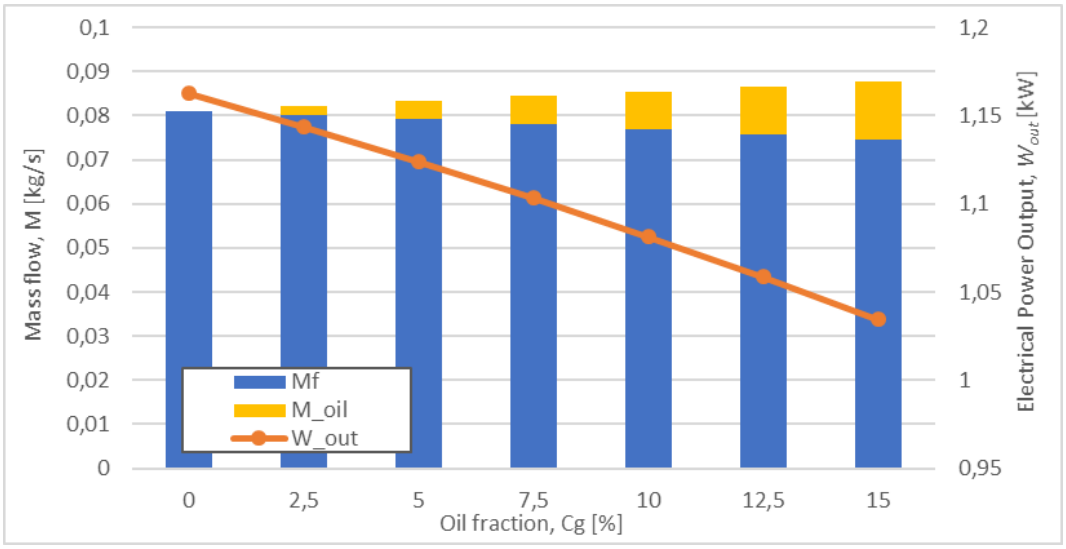

Figure 23 – Oil/ fluid mass flow rate and electrical power output as function of oil fraction.

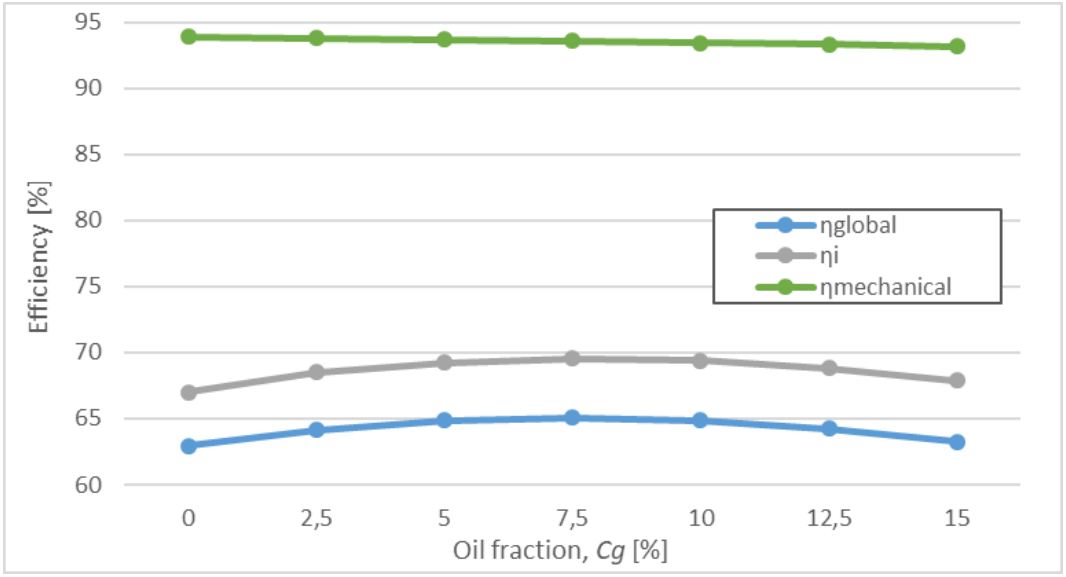

Figure 24 - Isentropic, mechanical and global efficiencies as function of oil fraction.

As can be observed, the electric energy output decreases with the increase of the oil fraction and the isentropic efficiency first increases and then diminishes with the increase oil fraction. This can be explained with the decrease of the mass flow of the fluid as the oil does not produce work, it is not considered for the thermodynamic process. The isentropic efficiency increases due to the reduction of the internal leakages in the expander. The mass flow rate decreases because the pressure ratio and other parameters are fixed, and the mass flow rate adapts in order to achieve the determined conditions.

The global efficiency reflects the isentropic and the mechanical (which is practically constant) efficiency and so its performance is also predictable. For instance, if the mass flow of the working fluid did not decrease, it would be expected the growth of the electric energy output.

As these results were not proven experimentally, a research in the literature was made in order to validate them. In Figure 25 are presented two charts based on the experimental results based on Dickes *et al*. [38] that show similar behaviours of the shown in this work. The filing factor presented in Figure 25 was not calculated for this study because it was not a relevant value for this analysis.

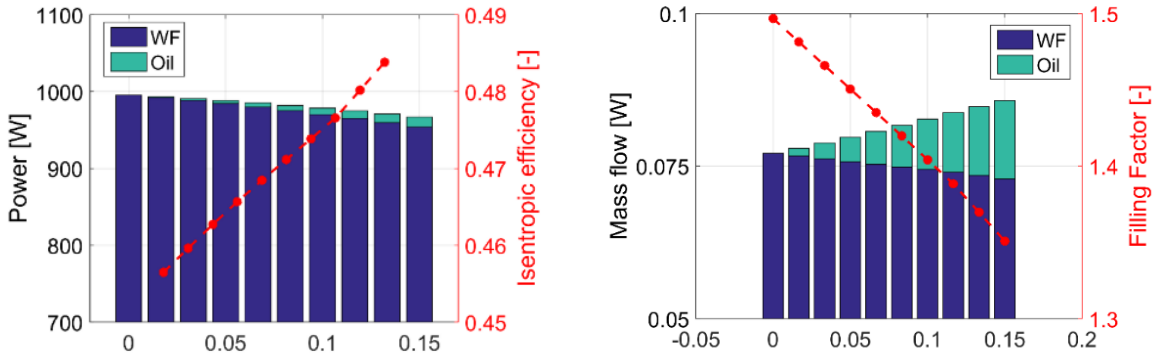

Figure 25 - Results of a similar cycle made by Dickes *et al.* [38].

Once the model of the expander is analysed individually, it will be proceeded a study of different ORC parameters influence in the expander. The inputs considering for the ORC model were the ones presented in Table 10.

Firstly, the isentropic efficiency and the specific electrical power output were extracted for a variation of the demand temperature (T_7), for different values of oil ratio, 2,5,

5 and 7,5% (shown in Figure 26). It is important to refer, as stated before, that one of the factors that reduces the electrical power output is the decrease of the organic fluid mass flow rate (see Figure 23). For this reason, in the following analysis will be studied the performance of the specific power output in order to avoid the influence of the referred reduction of the mass flow rate.

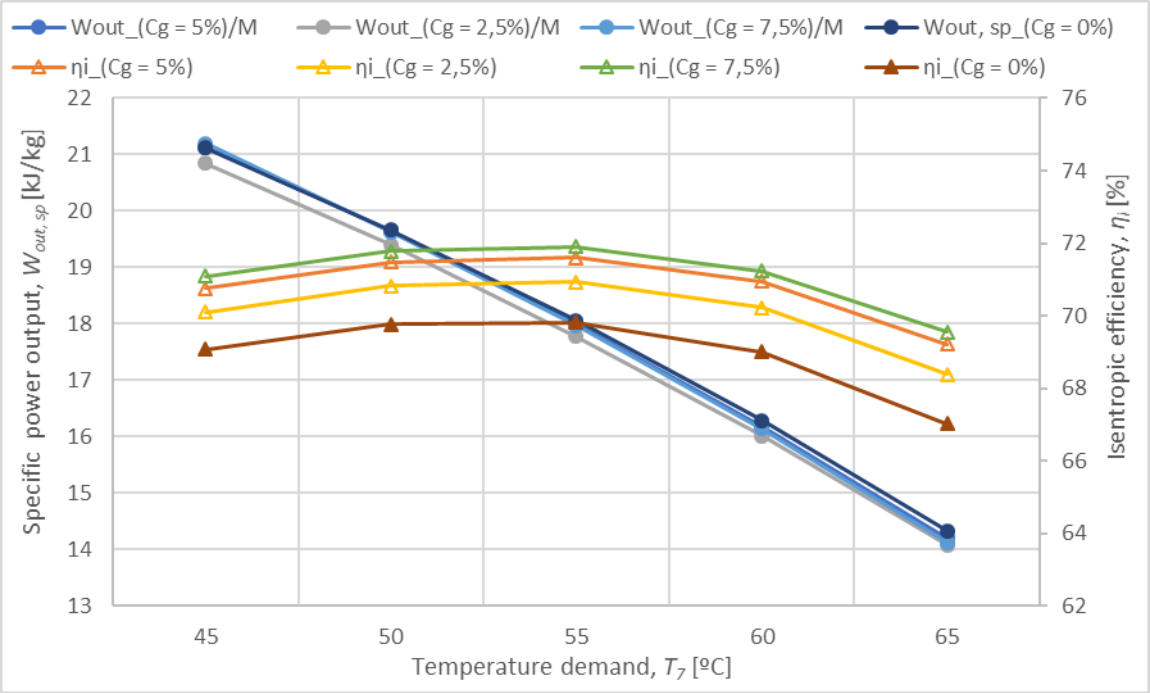

Figure 26 – Specific power output and isentropic efficiency as function of the temperature demand.

As can be observed in Figure 26, the isentropic efficiency has an optimum point for values of T_7 around 55ºC for every value of oil ratio. It is possible to achieve higher efficiencies for higher values of oil ratio. The specific electric power output decreases with the growth of demand temperature. This behaviour is expected because T_7 will influence the water temperature at the outlet of the condenser, if the value of Θ is fixed. As stated in the previous section, this temperature defines the minimum pressure of the system in order to avoid pinch point problems in the condenser. Taking this into account, with the increase of T_7, the minimum pressure of the system also growths and the pressure ratio will diminish (considering that the expander's inputs are fixed), and finally the specific power output will decrease.

Therefore, an analysis for different values of Θ was not proceeded, because its influence will be similar to the one presented with the variation of T_7. This means that the variations of the water temperature at the outlet of the condenser can be achieved by changing the demand temperature (T_7) or the values of Θ.

Afterwards, the system was analysed for different values of superheating degrees as shown in Figure 27.

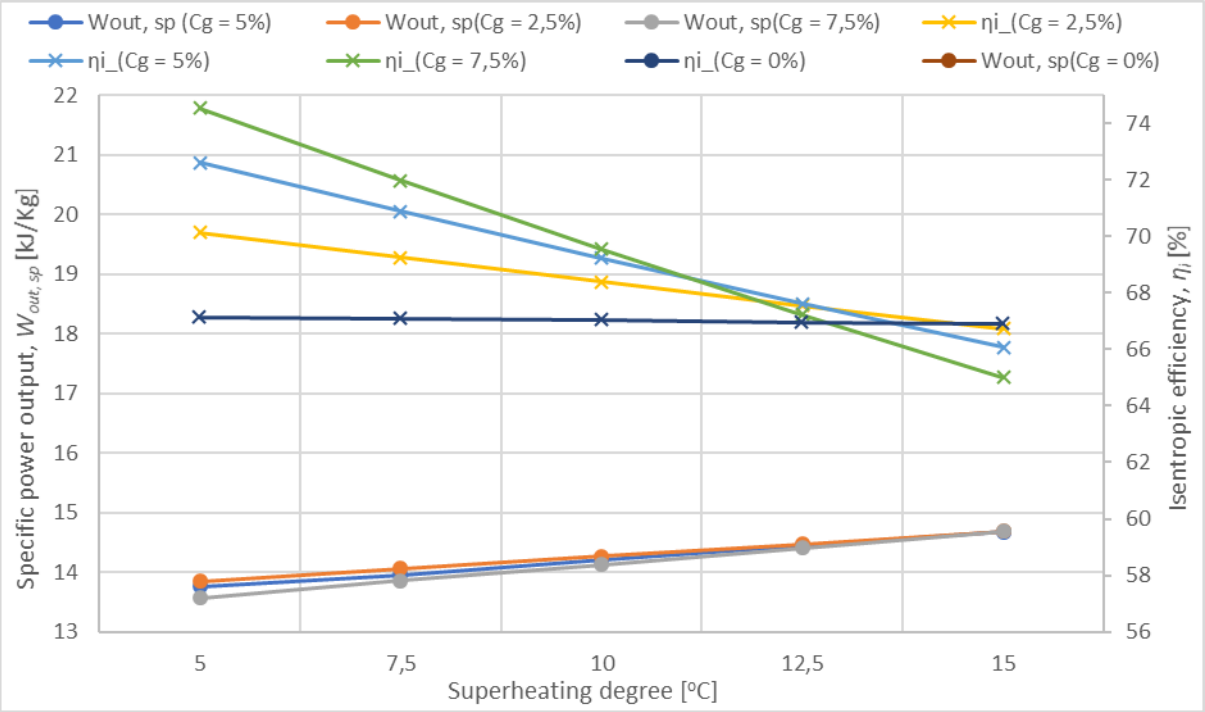

Figure 27 – Specific power output and isentropic efficiency as function of superheating degrees.

By observing Figure 27, it is possible to conclude that there is a slight increase of the specific power output with the growth of the superheating degree and the oil fraction barely influences its performance. This minor increase is due to the higher temperature (and not pressure) at the inlet of the expander that slightly changes the fluid transport proprieties and affect the process within it.

Regarding the isentropic efficiencies, there is a notable decrease with the increase of the superheating degree, and the oil ratio clearly influences its slope, especially for higher levels of oil ratio. This is due to the consideration of the oil proprieties in the mixture (the

oil is always at liquid phase and the fluid at gas state). This consideration is more noticeable for higher values of superheating degrees and higher values of oil fraction.

Finally, an analyse of the performance of the isentropic efficiency and the specific power output for different values of maximum pressure was made and the results are shown in Figure 28.

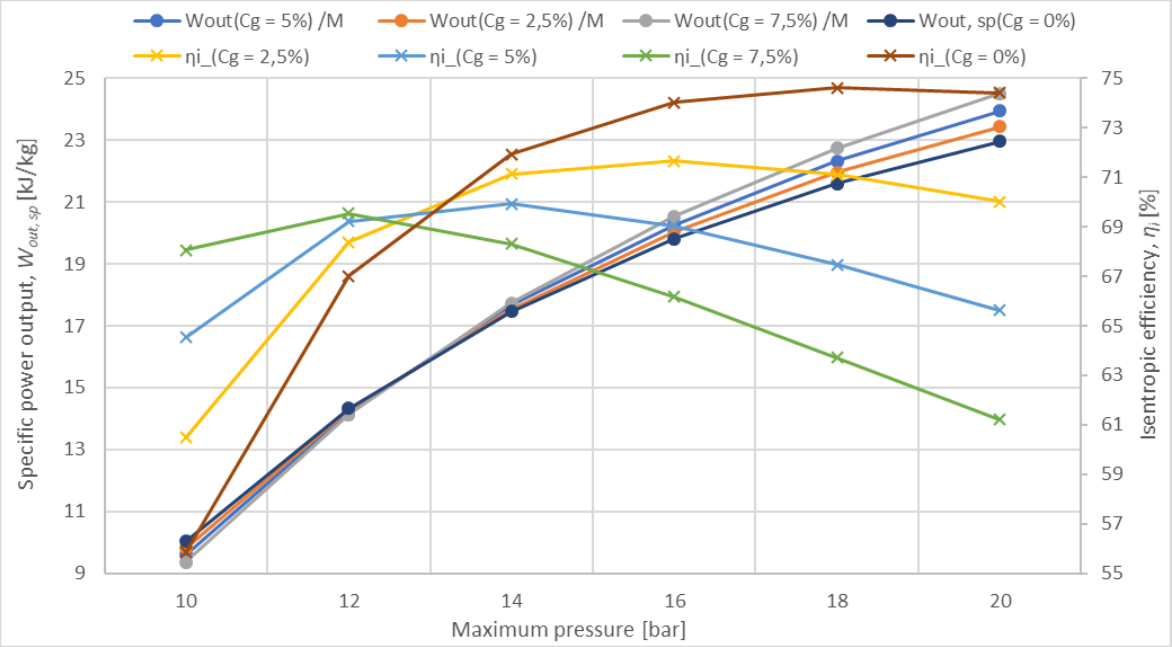

Figure 28 - Electric power output and isentropic efficiency for different values of maximum pressure.

As observed in Figure 28 there is a notable increase of the specific power output with the growth of the maximum pressure of the system. This can be mainly related with the fact that there is no established limit for the pressure ratio of the expander in order to achieve the determined conditions (once the minimal pressure of the system is fixed). From this the pressure ratio grows from around 2,6 (for 10 bar as maximum pressure) until 5,3 (for 20 bar as maximum pressure). Regarding the isentropic efficiencies, its optimal point evidently depends on the oil fraction which results in different values of the maximum pressure. It is also important to mention that the influence of the oil is not always constant along the increase of the maximum pressure. For instance, for lower values of maximum pressure increasing the oil fraction will increase the isentropic efficiency, however, after around 13 bar (in this case), increasing the oil fraction will decrease the isentropic efficiency. This happens because the influence of the oil is majorly felt on the losses (and leakages) of the

expander. Those values reach its superior limit for around 13 bar in this specific operating condition and also considering the physical characteristics of this expander (e.g.: the built-in volume ratio or the swept volume). This point is where the behaviour of isentropic efficiency along the oil fraction is reversed. For pressures above that point, increasing the oil fraction will only damaging its operation because the oil will not be contributing to produce work and will not reduce the losses (however, it is important to mention that its use is always recommended by the manufacturer due to operational and safety questions).

3.4. Updated test bench

The schematic diagram presented in Figure 29 presents the expander replacing the throttling valve and the lubrication system composed by an oil separator, a tank, a pump and finally a heat exchanger. It is important to refer that the sensors and control systems should also be applied, nevertheless this subject will be proposed to further investigations.

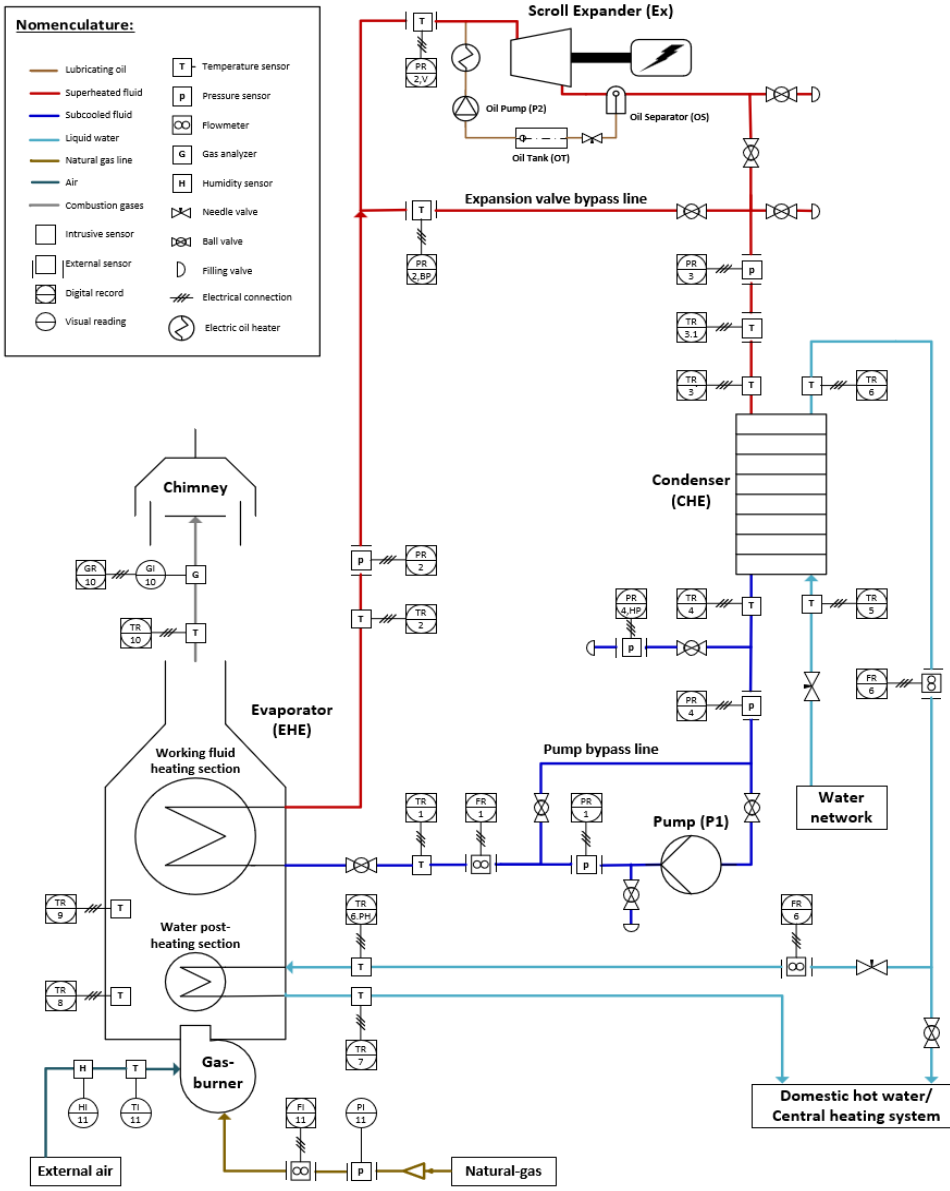

Figure 29 – Updated schematic diagram of the test bench (with expander and lubricating oil system).

4. FINAL REMARKS

4.1. Conclusions

The present study has four main topics: i) study and comparison of different types of expander available; ii) selection of the proper expander for the test bench that, for its turn, simulates a residential CHP system; iii) development of a simplified thermodynamic model of the ORC that includes the details of the expansion processes; and iv) design the implementation of the expander in a existent test bench, with the selection of the most relevant component.

Regarding the study and comparison of different expanders types and selection of the most appropriate for this application, a research was carried out where it was concluded that between positive displacement expanders and turbines, the positive displacement expanders were the suitable option for a domestic scale. This is due to their low cost, simplicity, low rotational speeds and tolerance to two phase flows. From the volumetric expanders, there were four types that stood out: scroll, screw, piston and rotary vane. After a comparison study it was settled that the hermetic scroll expander was the most appropriate for household applications due to its compactness, high (and regular) isentropic efficiencies, low production costs and lower power outputs (1-5 kW) which are the desirable characteristics. However, it was noticed one drawback that is its need for lubrication.

Based on the existent test bench based in DEM-UC a simple thermodynamic model was developed to study the ORC system and a semi-empirical model for the expander. The expander ZR61KRE-TDF from Copeland was selected and its technical data was applied in the semi-empirical model. Nevertheless, there were some important data missing and other methodologies was applied in order to achieve the information required to run the model.

When referring the lubrication of the expander, two options were presented: i) the oil flows through the complete ORC system, mixing with the organic fluid; and, ii) the oil only circulates in the expander section, by implementing an oil separator after the expander

where the oil will be separated from the working fluid and pumped again into the expander. The impact of the lubrication in the components of the ORC system is often neglected by the community. Due to the uncertainty of this option, a simple research was made in order to understand the influence of the lubricating oil in the system. It was concluded that the overall efficiency of the ORC decreases. Another aspect to consider is the fact that the lubricating oil flowing in the components can be trapped and hot spots may occur, especially in the evaporator. As the evaporator in the test bench uses direct vaporization, the circulation of oil can be dangerous. So, it was decided to implement the option two (external oil cycle) to lubricate the expander.

After this decision, the lubricating oil proprieties are added to the expander model. For this, another methodology was used in order to estimate the oil-fluid mixture thermodynamic characteristics.

Finally, a parametrical analysis of the main inputs of the model was conducted, in order to understand theirs influences to the operation of the expander. It was concluded that the increase of the oil ratio, the mass flow of the fluid decreases and the mixture mass flow increases. With this, the power output decreases since the oil does not produces work in the expansion process. However, the isentropic efficiency increases because the oil reduces the internal leakages. Higher temperature demands increase the minimum pressure value, the pressure ratio will decrease, and the specific power output will decrease. Regarding the super heating degree increase, the isentropic efficiencies decreases, and the oil ratio influences its slope. Analysing different values of maximum pressure, there is a notable growth of the specific power output with the increase of the maximum pressure and this behaviour can be explained by the fact that there is no limit established for the pressure ratio in order to achieve the determined conditions.

Lastly, some options regarding the necessary components of the external oil circuit were presented as well as a final schematic diagram of the entire system, containing this external circuit and the referred expander.

4.2. Future work

For the future, as previously mention, it would be recommended to implement a liquid receiver after the condenser. After analysing several systems, it was noticed a presence of a liquid receiver. According to some studies [10,11,13,21], the implementation of a liquid receiver after the condenser is recommended, so it ensures a saturated liquid at the condenser outlet is possible to adjust the refrigerant level in the circuit. This way, the variations of the liquid level in the heat exchangers are compensated by a variation of the liquid level in the liquid receiver. Another advantage presented is in the start-up of the ORC system the pump might cavitate which is not advisable. The liquid receiver assures there is liquid refrigerant flowing in the pump and guarantees the required net positive suction head (NPSH) in this stage. In principle, the dimensioning of this component should be simple, however, there may be some questioning about its installation and position in the test bench.

Another question emerging from this study was the electrical energy dissipation. As the expander produces electrical energy, this needs to be directed to the greed or to a dissipation system. As this application is for a test bench an implementation of some resistances to dissipate the electrical energy would be recommended. Additionally, it is also important to evaluate the direction of the current. Perhaps in the start-up of the system, the expander might need some electrical energy, before starts producing it.

Finally, the proper instrumentation must be also selected and implemented in order to measure the proprieties of the system in some important points in order to experimentally validate the model developed through this thesis and to support the control of the cycle at the desired operating conditions.

REFERENCES

[1] Greenhouse gases - U.S. Energy Information Administration (EIA) https://www.eia.gov/energyexplained/energy-and-the-environment/greenhouse-gases.php (accessed August 29, 2022).

[2] Atmospheric Carbon Dioxide Levels Reach New High | Scripps Institution of Oceanography https://scripps.ucsd.edu/news/atmospheric-carbon-dioxide-levels-reach-new-high (accessed August 29, 2022).

[3] How have CO2 levels changed since the industrial revolution? | World Economic Forum https://www.weforum.org/agenda/2021/03/met-office-atmospheric-co2-industrial-levels-environment-climate-change/ (accessed August 29, 2022).

[4] Pereira JS, Ribeiro JB, Mendes R, Vaz GC, André JC. ORC based micro-cogeneration systems for residential application - A state of the art review and current challenges. Renew Sustain Energy Rev 2018;92:728–43. https://doi.org/10.1016/j.rser.2018.04.039.

[5] Bianchi M, Branchini L, De Pascale A, Peretto A. Application of environmental performance assessment of CHP systems with local and global approaches. Appl Energy 2014;130:774–82. https://doi.org/10.1016/J.APENERGY.2014.04.017.

[6] Angrisani G, Roselli C, Sasso M. Distributed microtrigeneration systems. Prog Energy Combust Sci 2012;38:502–21. https://doi.org/10.1016/J.PECS.2012.02.001.

[7] Energy statistics - an overview - Statistics Explained https://ec.europa.eu/eurostat/statistics-explained/index.php?title=Energy_statistics_-_an_overview#Final_energy_consumption (accessed August 29, 2022).

[8] Maghanki MM, Ghobadian B, Najafi G, Galogah RJ. Micro combined heat and power (MCHP) technologies and applications. Renew Sustain Energy Rev 2013;28:510–24. https://doi.org/10.1016/J.RSER.2013.07.053.

[9] Pedro J. S TUDY AND DEVELOPMENT OF EVAPORATORS FOR RESIDENTIAL - SCALE COGENERATION SYSTEMS BASED ON 2021.

[10] Quoilin S. 21_Sustainable Energy Conversion Through the Use of Organic Rankine Cycles for Waste Heat Recovery and Solar Applications, Sylvain Quoilin, University of Liège, Belgium, 2008 2011.

[11] Dumont O. Investigation of a heat pump reversible into an organic Rankine cycle and its application in the building sector. Thesis 2017:236.

[12] Usman M, Imran M, Haglind F, Pesyridis A, Park BS. Experimental analysis of a micro-scale organic Rankine cycle system retrofitted to operate in grid-connected mode. Appl Therm Eng 2020;180:115889. https://doi.org/10.1016/j.applthermaleng.2020.115889.

[13] Eyerer S, Dawo F, Altnöder M, Windhager R, Esch H, Ausfelder S, et al. Design and First Operation of an Advanced Orc-Chp Architecture. 5th Int Semin ORC Power Syst 2019:1–10.

[14] Wajs J, Mikielewicz D, Bajor M, Kneba Z. Experimental investigation of domestic micro-CHP based on the gas boiler fitted with ORC module. Arch Thermodyn 2016;37:79–93. https://doi.org/10.1515/aoter-2016-0021.

[15] Richter L. ORC test rig with a screw expander; Design and expectations. AIP Conf Proc 2018;2047. https://doi.org/10.1063/1.5081652.

[16] Pereira JS, Santos M, Mendes R, André JC, Ribeiro JB. Thermal degradation assessment study of a direct vaporization ORC based micro-CHP system under close-to-real operating conditions. Appl Therm Eng 2022;214:118878. https://doi.org/10.1016/J.APPLTHERMALENG.2022.118878.

[17] Dawo F, Fleischmann J, Kaufmann F, Schifflechner C, Eyerer S, Wieland C, et al. R1224yd(Z), R1233zd(E) and R1336mzz(Z) as replacements for R245fa: Experimental performance, interaction with lubricants and environmental impact. Appl Energy 2021;288. https://doi.org/10.1016/j.apenergy.2021.116661.

[18] Moradi R, Habib E, Bocci E, Cioccolanti L. Component-Oriented Modeling of a Micro-Scale Organic Rankine Cycle System for Waste Heat Recovery Applications. Appl Sci 2021;11:1984. https://doi.org/10.3390/app11051984.

[19] Weller T, Jockenhöfer H, Fiss M, Bauer D. Detailed design of the ORC laboratory

prototype Type 2020.

[20] Eyerer S, Dawo F, Kaindl J, Wieland C, Spliethoff H. Experimental investigation of modern ORC working fluids R1224yd(Z) and R1233zd(E) as replacements for R245fa. Appl Energy 2019;240:946–63. https://doi.org/10.1016/j.apenergy.2019.02.086.

[21] Galindo J, Ruiz S, Dolz V, Royo-Pascual L, Haller R, Nicolas B, et al. Experimental and thermodynamic analysis of a bottoming Organic Rankine Cycle (ORC) of gasoline engine using swash-plate expander. Energy Convers Manag 2015;103:519–32. https://doi.org/10.1016/j.enconman.2015.06.085.

[22] Qiu G, Liu H, Riffat S. Expanders for micro-CHP systems with organic Rankine cycle. Appl Therm Eng 2011;31:3301–7. https://doi.org/10.1016/j.applthermaleng.2011.06.008.

[23] Isabirye M, Raju DV., Kitutu M, Yemeline V, Deckers J, J. Poesen Additional. We are IntechOpen , the world ' s leading publisher of Open Access books Built by scientists , for scientists TOP 1 %. Intech 2012:13.

[24] Zywica G, Kaczmarczyk TZ, Ihnatowicz E. A review of expanders for power generation in small-scale organic Rankine cycle systems: Performance and operational aspects. Proc Inst Mech Eng Part A J Power Energy 2016;230:669–84. https://doi.org/10.1177/0957650916661465.

[25] Dumont O, Talluri L, Fiaschi D, Manfrida G, Lemort V. Comparison of a scroll, a screw, a roots, a piston expander and a Tesla turbine for small-scale organic Rankine cycle. 5 Th Int Semin ORC Power Syst 2019:1–8.

[26] Pardinas AA, Pilarczyk M, Agromayor R, Nord LO. Design of an Experimental ORC Expander Setup Using Natural Working Fluids. Asme Orc2019 2017;43:1–8.

[27] Reciprocating Compressors Working, Applications, Advantages and Disadvantages | Mecholic https://www.mecholic.com/2019/03/reciprocating-compressors-working.html (accessed October 2, 2022).

[28] Pereira JS, Almeida J, André JC, Mendes R, Ribeiro JB. Modelling and experimental validation of the heat-transfer processes of a direct vaporization micro-scale ORC-evaporator for thermal degradation risk assessment. Energy Convers Manag

2021;238. https://doi.org/10.1016/j.enconman.2021.114130.

[29] Lemmon, E.; McLinden, M.O., Huber ML. NIST reference fluid thermodynamic and transport properties-REFPROP. … Chem Prop … 2002;23:v7.

[30] Pereira JS, Ribeiro JB, Mendes R, André JC. Analysis of a hybrid (topping/bottoming) ORC based CHP configuration integrating a new evaporator design concept for residential applications. Appl Therm Eng 2019;160:113984. https://doi.org/10.1016/j.applthermaleng.2019.113984.

[31] Lemort V, Quoilin S, Cuevas C, Lebrun J. Testing and modeling a scroll expander integrated into an Organic Rankine Cycle. Appl Therm Eng 2009;29:3094–102. https://doi.org/10.1016/j.applthermaleng.2009.04.013.

[32] Lemort V, Declaye S, Quoilin S. Experimental characterization of a hermeti scroll expander for use in a micro-scale Rankine cycle. Proc Inst Mech Eng Part A J Power Energy 2012;226:126–36. https://doi.org/10.1177/0957650911413840.

[33] Giuffrida A. Modelling the performance of a scroll expander for small organic Rankine cycles when changing the working fluid. Appl Therm Eng 2014;70:1040–9. https://doi.org/10.1016/j.applthermaleng.2014.06.004.

[34] Dickes R, Dumont O, Bell IH, Declaye S, Quoilin S, Bell I. Experimental investigation of an ORC system for a micro-solar power plant Energy management View project Dispa-SET View project Experimental investigation of an ORC system for a micro-solar power plant 2014.

[35] Dickes R, Dumont O, Guillaume L, Quoilin S, Lemort V. Charge-sensitive modelling of organic Rankine cycle power systems for off-design performance simulation. Appl Energy 2018;212:1262–81. https://doi.org/10.1016/J.APENERGY.2018.01.004.

[36] Feng Y qiang, Hung TC, He YL, Wang Q, Chen SC, Wu SL, et al. Experimental investigation of lubricant oil on a 3 kW organic Rankine cycle (ORC) using R123. Energy Convers Manag 2019;182:340–50. https://doi.org/10.1016/J.ENCONMAN.2018.12.021.

[37] Moradi R, Villarini M, Habib E, Bocci E, Colantoni A, Cioccolanti L. Impact of the expander lubricant oil on the performance of the plate heat exchangers and the scroll

expander in a micro-scale organic Rankine cycle system. Appl Therm Eng 2021;189:116714. https://doi.org/10.1016/j.applthermaleng.2021.116714.

[38] Dickes R. Charge-sensitive methods for the off-design performance characterization of organic Rankine cycle (ORC) power systems 2019.

[39] Moradi R, Villarini M, Habib E, Bocci E, Colantoni A, Cioccolanti L. Impact of the expander lubricant oil on the performance of the plate heat exchangers and the scroll expander in a micro-scale organic Rankine cycle system. Appl Therm Eng 2021;189. https://doi.org/10.1016/j.applthermaleng.2021.116714.

[40] Selecting, Installing Oil Separators | ACHR News n.d. https://www.achrnews.com/articles/91004-selecting-installing-oil-separators (accessed September 26, 2022).

[41] AC&R Components. Helical Oil Separators 2005:10–1.

[42] Peristaltic Pumps Selection Guide: Types, Features, Applications | Engineering360 https://www.globalspec.com/learnmore/flow_transfer_control/pumps/peristaltic_pumps (accessed October 1, 2022).

[43] Jia X, Wang J, Wang X, Hu Y, Sun Y. Phase equilibrium of R1234yf and R1234ze(E) with POE lubricant and thermodynamic performance on the evaporator. Fluid Phase Equilib 2020;514:112562. https://doi.org/10.1016/j.fluid.2020.112562.

[44] Morais ARC, Simoni LD, Shiflett MB, Scurto AM. Viscosity and Density of an ISO VG 32 Polyol Ester Lubricant Saturated with Compressed Hydrofluorocarbon Gases: R-134a, R-32, and R-125. J Chem Eng Data 2022. https://doi.org/10.1021/acs.jced.2c00139.

[45] Dickes R, Dumont O, Lemort V. Lubricating oil entrainment in an ORC system and its impact on performance rating. 5th Annu Engine ORC Consort Work Automot Station Engine Ind 2018:25–7.

ANNEX A

ELEKTRONIKA SA.
TECHNIKA CHŁODNICZA I KLIMATYZACJA

Model: ZR61KCE-TFD
Data

Type: Hermetic scroll compressors
Producer: Copeland
Series: ZR

Model: ZR61KCE-TFD

Technical data

Displacement [m³/h]:	14,4
Sound power [dBA]:	71
Sound pressure level [dB]:	60
Net Weight [kg]:	36,1
Oil charge [dm³]:	2,0
Maximum high pressure [bar]:	29,5
Maximum standstill pressure [bar]:	20
Maximum lowside temperature [°C]:	50
PED category:	1

Electrical data

Power supply [V/~/Hz]:	380-420/3/50Hz
Locked rotor current [A]:	65,5
Max. operating current [A]:	11,0
Winding resistance [Ω]:	2,8

Connections

	inches
Suction Rotolock valve connection:	1 1/4"
Discharge Rotolock valve connection:	1"
Suction connection with supplied sleeve:	7/8"
Discharge connection with supplied sleeve:	1/2"

R134a

Cooling capacity [kW]

t_c \ t_e	-20	-15	-10	-5	0	5	10	15
30	3.46	4.55	5.80	7.27	8.99	11.00	13.34	-
35	3.24	4.29	5.49	6.90	8.54	10.47	12.72	-
40	3.02	4.03	5.18	6.53	8.10	9.94	12.09	14.58
45	-	3.77	4.87	6.15	7.65	9.40	11.45	13.83
50	-	3.51	4.55	5.77	7.18	8.85	10.79	13.06
55	-	-	4.23	5.37	6.71	8.28	10.13	12.28
60	-	-	-	4.96	6.22	7.70	9.44	11.47
65	-	-	-	4.54	5.71	7.09	8.72	10.64
70	-	-	-	-	5.18	6.46	7.98	9.78
75	-	-	-	-	4.62	5.80	7.21	8.89

Power input [kW]

t_c \ t_e	-20	-15	-10	-5	0	5	10	15
30	1.67	1.71	1.73	1.75	1.76	1.78	1.80	-
35	1.86	1.90	1.93	1.95	1.96	1.98	2.01	-
40	2.07	2.11	2.14	2.16	2.18	2.20	2.24	2.28
45	-	2.35	2.38	2.40	2.42	2.45	2.48	2.53
50	-	2.62	2.65	2.67	2.69	2.71	2.75	2.79
55	-	-	2.96	2.98	2.99	3.01	3.05	3.09
60	-	-	-	3.32	3.34	3.35	3.38	3.42
65	-	-	-	3.72	3.73	3.74	3.76	3.80
70	-	-	-	-	4.17	4.17	4.19	4.22
75	-	-	-	-	4.67	4.66	4.67	4.70

Current [A]

t_c \ t_e	-20	-15	-10	-5	0	5	10	15
30	5.05	5.10	5.12	5.13	5.12	5.12	5.13	-
35	5.08	5.15	5.19	5.20	5.21	5.21	5.22	-
40	5.18	5.27	5.33	5.36	5.37	5.38	5.39	5.43
45	-	5.48	5.55	5.59	5.61	5.62	5.64	5.67
50	-	5.75	5.84	5.89	5.92	5.94	5.96	5.99
55	-	-	6.20	6.26	6.30	6.33	6.35	6.38
60	-	-	-	6.70	6.75	6.78	6.81	6.84
65	-	-	-	7.21	7.27	7.30	7.33	7.36
70	-	-	-	-	7.84	7.89	7.92	7.95
75	-	-	-	-	8.48	8.53	8.56	8.59

Mass flow [kg/h]

t_c \ t_e	-20	-15	-10	-5	0	5	10	15
30	81.49	105.18	131.67	161.69	195.93	235.12	279.97	-
35	80.46	104.16	130.65	160.64	194.84	233.97	278.75	-
40	79.50	103.22	129.70	159.66	193.82	232.89	277.58	328.61
45	-	102.22	128.69	158.62	192.73	231.74	276.35	327.28
50	-	101.05	127.50	157.40	191.47	230.40	274.93	325.75
55	-	-	126.02	155.89	189.90	228.76	273.20	323.92
60	-	-	-	153.95	187.90	226.69	271.04	321.65
65	-	-	-	151.47	185.37	224.08	268.33	318.83
70	-	-	-	-	182.16	220.80	264.95	315.33
75	-	-	-	-	178.17	216.72	260.77	311.04

C.O.P. [W/W]

t_c \ t_e	-20	-15	-10	-5	0	5	10	15
30	2.07	2.66	3.35	4.16	5.10	6.18	7.39	-
35	1.74	2.26	2.85	3.54	4.35	5.28	6.31	-
40	1.46	1.91	2.42	3.02	3.71	4.51	5.40	6.39
45	-	1.60	2.05	2.56	3.16	3.84	4.62	5.47
50	-	1.34	1.72	2.16	2.67	3.26	3.93	4.68
55	-	-	1.43	1.81	2.24	2.75	3.33	3.97
60	-	-	-	1.49	1.86	2.30	2.79	3.35
65	-	-	-	1.22	1.53	1.90	2.32	2.80
70	-	-	-	-	1.24	1.55	1.91	2.32
75	-	-	-	-	0.99	1.24	1.54	1.89

Application range

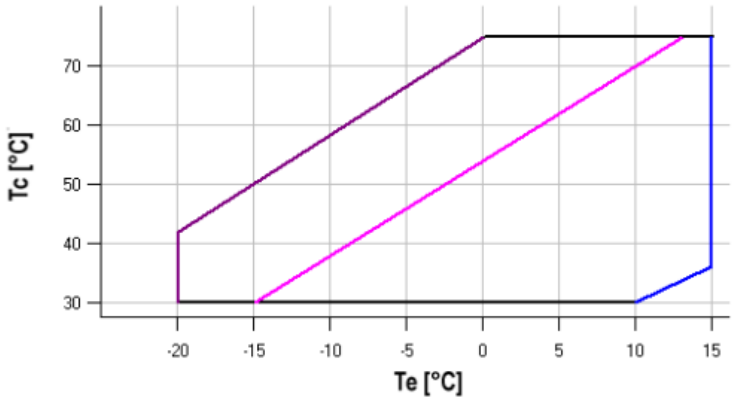

Maximum evaporating temperature
25°C suction gas temperature
10K gas overheat

Operating conditions: 10K suction superheat, 0K subcooling
t_c - Condensing temperature [°C]
t_e - Evaporating temperature [°C]

APPENDIX A

The appendix is in a Google sheets table that can be accessed in the following link during the next five years.
https://docs.google.com/spreadsheets/d/1vqYh65M-YXdKuvwcMj-w6baYW-UMcQGCEqahqRPsrJo/edit?usp=sharing